5-1-1995

Phenomenologial Dynamics of C_{70}

Ravi Sachidanandam
University of Pennsylvania

Tom C. Lubensky
University of Pennsylvania, tom@physics.upenn.edu

A. Brooks Harris
University of Pennsylvania, harris@sas.upenn.edu

Phenomenologial Dynamics of C$_{70}$

Abstract

We construct the most general effective Hamiltonian for the C$_{70}$ solid and study the long-wavelength dynamics of the system near the high-temperature orientational ordering phase transition. We derive neutron scattering cross sections, NMR line shifts, and T$_1$ from our theory and suggest some experiments to further constrain our Hamiltonian.

Disciplines

Physics

Phenomenological dynamics of C$_{70}$

R. Sachidanandam, T. C. Lubensky, and A. B. Harris

Department of Physics, University of Pennsylvania, Philadelphia, Pennsylvania 19104

(Received 29 September 1994)

We construct the most general effective Hamiltonian for the C$_{70}$ solid and study the long-wavelength dynamics of the system near the high-temperature orientational ordering phase transition. We derive neutron scattering cross sections, NMR line shifts, and T_1 from our theory and suggest some experiments to further constrain our Hamiltonian.

I. INTRODUCTION

The fullerene molecules C$_n$ are an intriguing family. The most celebrated member of this family is C$_{60}$, which forms a replica on a microscopic scale of a soccer ball.[1] Not long after the discovery of this molecule, its crystal structure in the solid state was investigated. At temperatures well above room temperature, solid C$_{60}$ consists of orientationally disordered molecules whose centers form a fcc lattice,[2] but at a temperature of about 250 K it undergoes a transition[3] to a long-range orientationally ordered structure with four orientationally inequivalent molecules per simple cubic unit cell and identified as belonging to space group $Pa3$.[4–7] This phase transition is discontinuous[8,9] in agreement with the predictions of Landau theory[10] or mean-field theory[11,12] based on various intermolecular potentials. The energies of the orientational elementary excitations (librons) in the orientationally ordered phase, determined via inelastic neutron scattering,[13] agree qualitatively with calculations[14,15] based on recent models[16,17] for the intermolecular orientational interactions. The evolution of the orientational elementary excitations as the temperature passes through the phase transition has been the object of some experimental work,[13] but due to the complicated nature of the order parameter,[10,11] no detailed study of the dynamics has been made.

The next most widely studied fullerene is C$_{70}$. For some purposes the C$_{70}$ molecule may be modeled as an ellipsoid of revolution. At high temperatures, solid C$_{70}$ shows no long-range orientational order of its molecules, and its crystal structure is the same as that of orientationally disordered C$_{60}$.[18] As the temperature is lowered through a critical value, $T_>$, there is a phase transition to a phase with long-range orientational order[19,20] of the molecules. In this new phase (which we will refer to as the intermediate phase), the long axes of all the molecules align, on average, along one of the fcc lattice's threefold axes [the four (1,1,1) directions], but the molecules continue to spin about their long axes. The development of long-range orientational order breaks cubic symmetry and, as a result,[21,22] the crystal distorts into a rhombohedral lattice.[19,20] Experimental studies show that this phase transition is discontinuous with a latent heat comparable to that of C$_{60}$.[23,24] Molecular dynam-

ics calculations[25] have reproduced the discontinuous nature of this transition, and a later Landau analysis[21] confirmed that this behavior does not depend on the details of the orientational potential used. (For a mean-field analysis based on microscopic potentials see Callebaut and Michel.[22]) Although the difficulty in sample preparation has so far prevented measurements of the libron spectrum of single crystals, recent inelastic neutron scattering experiments[26] on powder samples indicate some of the main features of the dynamics at temperatures near $T_>$.

At a temperature $T_<$, somewhat below $T_>$, the molecules appear to stop spinning.[18,19,27] Because of the fivefold symmetry of the molecule, the resulting more completely ordered phase can no longer have rhombohedral symmetry. It is believed that the crystal structure is monoclinic,[18] but the space group for this phase has not been determined. Molecular dynamics[25] does predict a second transition, but probably because the orientational potential is not well enough known, the crystal structure predicted is incompatible with x-ray data[18] for $T < T_<$. The orientational order parameter, which describes the ordered phase below $T_<$, was discussed elsewhere.[21] Since the experimental information about this phase is rather vague at present, we will not consider it any further here. Information concerning the two orientational ordering transitions is summarized in Fig. 1.

Until now the orientational dynamics of the fullerenes has received little theoretical attention. Some information can be obtained from molecular dynamics simulations,[25] but such numerical studies have some limitations. For instance, they have difficulty in probing the dynamical response in the long-wavelength limit. In addition, such studies do not readily indicate which results are a consequence of symmetry and which are model dependent. On the other hand, in principle, molecular dynamics simulations do properly include the effects of fluctuations. However, qualitatively correct results which elucidate the role of symmetry can be obtained using a phenomenological theory. Accordingly, in this paper we develop a phenomenological treatment of the orientational dynamics of solid C$_{70}$ at temperatures near the high-temperature phase transition. For this purpose we construct an effective Hamiltonian to treat long-wavelength fluctuations. As mentioned above,

Low Temperature Phase.	Intermediate Phase	High Temperature Phase
T< 280 K	280 K < T < 340 K	T>340 K
MONOCLINIC	RHOMBOHEDRAL	FCC
Molecular orientations ordered, but the orientational structure is not known.	The long axes of all molecules lie along the rhombohedral axis. Molecules spin about the long axis.	Molecular orientations disordered

FIG. 1. A schematic representation of the phase diagram of solid C$_{70}$. We indicate the orientational ordering of the molecules and the crystal symmetry for different temperature ranges.

FIG. 2. The C$_{70}$ molecule with its fivefold rotation axis along the z axis, the horizontal mirror in an x-y plane, and a vertical mirror in a y-z plane.

we recently presented a mean-field Landau expansion for the static free energy which demonstrates, on the basis of symmetry only, that the higher-temperature transition is discontinuous. This static free energy represents the zero-wave-vector and zero-frequency limit of the effective Hamiltonian we require to treat the dynamics. Our treatment of the dynamics explains various experimental results and provides guidance for future studies.

Briefly, this paper is organized as follows. In Sec. II we construct a free energy for the system and review its static equilibrium properties. In Sec. III we obtain the equations of motion from a Hamiltonian based on the static free energy. Section IV deals with the consequences for neutron scattering experiments from our theory. In Sec. V we discuss the consequences of our theory for NMR studies. In the final section we summarize our conclusions and suggest some experimental tests for our theory.

II. STATICS

We now discuss briefly a mean-field theory for the static description of the phase transition based on previous work.[21] We describe the C$_{70}$ molecule and define an order parameter for the intermediate ordered phase. Using this order parameter we find quantities that are invariant under the symmetry operations of the high-temperature cubic phase and use them to construct a free energy for the system. We discuss the consequences of this free energy for the static equilibrium properties and set the stage for extension of this to describe dynamics in this system.

A. Molecule and the order parameter

C$_{70}$ is a cigar-shaped molecule with D_{5h} symmetry,[28] as shown in Fig. 2. The fivefold axis of the molecule is its
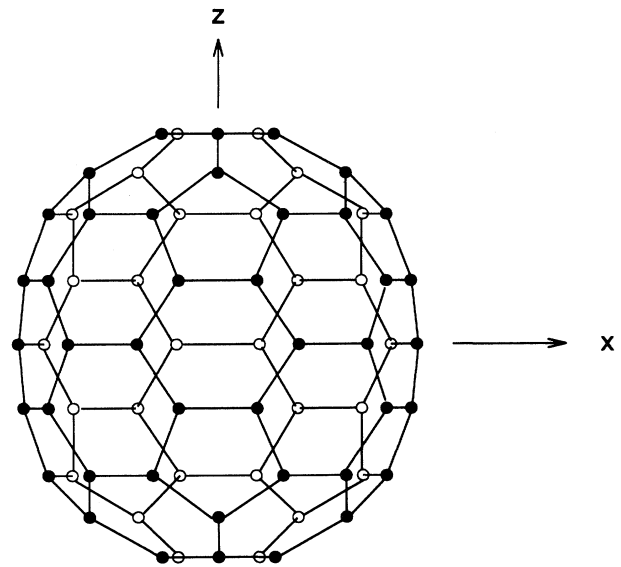
long axis. It has a horizontal mirror plane perpendicular to the long axis and five other mirror planes containing this axis. If the molecule spins about its long axis, then effectively it has $D_{\infty h}$ symmetry.

In the solid, at high temperatures ($T > T_> \approx 300$ K) the molecules are centered at the sites of a fcc lattice (space group $Fm\bar{3}m$) and there is no long-range orientational order. As the temperature is reduced below $T_>$, a phase transition occurs. The molecules continue to spin about their long axes, which align parallel to each other along one of the threefold axes (111 direction) of the fcc lattice. This orientational ordering transition breaks the cubic symmetry and leaves a single threefold axis along the average direction of the long axes of the molecules (space group $R\bar{3}$). There is an accompanying distortion[21,22] of the lattice from fcc to a rhombohedral.

The first step in developing a theory for a phase transition is the definition of an order parameter that is zero in the disordered phase and nonzero in the ordered phase. In C$_{70}$ inversion should leave the order parameter invariant since the molecule itself has inversion symmetry in this phase. Thus an appropriate order parameter, for the transition to the intermediate phase in C$_{70}$, is identical to the one defined for nematic liquid crystals.[29] Let $\nu(\mathbf{1})$ be the unit vector along the long axis of the molecule, at site 1. Thus,

$$\nu(\mathbf{1}) = (\sin\theta(\mathbf{1})\cos\phi(\mathbf{1}), \quad \sin\theta(\mathbf{1})\sin\phi(\mathbf{1}), \quad \cos\theta(\mathbf{1})),$$
$$(2.1)$$

where $\theta(\mathbf{1})$ and $\phi(\mathbf{1})$ are the spherical angles specifying the orientation of the long axis of the molecule at site 1. The simplest order parameter characterizing the orientational order in the intermediate phase is then

$$Q_{ij}(\mathbf{1}) = \langle \nu_i(\mathbf{1})\nu_j(\mathbf{1}) - \tfrac{1}{3}\delta_{ij} \rangle , \qquad (2.2)$$

where ν_i refers to the ith component of ν and $\langle \ \rangle$ indicates an ensemble average. In general, higher-order tensors, equivalent to $\langle Y_L^M(\theta, \phi)\rangle$ with $L > 2$, or higher-order symmetry-adapted functions[11,12,22] are necessary for a complete description of the orientational probability distribution. However, the theory we develop here is that which would result when these higher-order functions have been integrated out to give an effective theory in terms of only the Q_{ij}'s. This theory has the correct symmetry and correctly describes all the low-energy modes. However, since it is a phenomenological model, the constants appearing in the free energy can only be evaluated from a detailed micoscopic calculation. In the absence of such a calculation we will estimate these constants by relating them to experimentally accessible quantities.

We restrict attention to the hydrodynamic (i.e., small $\mathbf{k}, \omega$) limit for the purpose of studying the mean-field properties. Since we are interested primarily in long-wavelength excitations, we find it convenient to deal with an order parameter

$$Q_{ij}(\mathbf{r}, t) = \frac{1}{n} \sum_l Q_{ij}(\mathbf{l}, t)\delta(\mathbf{r} - \mathbf{l}), \qquad (2.3)$$

defined at points $\mathbf{r}$ in space rather than $Q_{ij}(\mathbf{l})$ defined at sites $\mathbf{l}$. Here n is the number of molecules per unit volume. $Q_{ij}(\mathbf{r}, t)$ is a dimensionless, traceless, and symmetric tensor. It is always possible to find a local coordinate system in which it is diagonal and is of the form

$$Q = \frac{1}{3}\begin{pmatrix} -S + \eta & 0 & 0 \\ 0 & -S - \eta & 0 \\ 0 & 0 & 2S \end{pmatrix}, \qquad (2.4)$$

where S is the uniaxial and η is the biaxial order parameter which is usually chosen so that $|\eta| < |S|$. In the intermediate equilibrium state there is uniaxial order with $\eta = 0$, and we may write

$$\langle Q_{ij}(\mathbf{r}, t)\rangle = S(\mathbf{r}, t)\left(n_i(\mathbf{r})n_j(\mathbf{r}) - \frac{1}{3}\delta_{ij}\right), \qquad (2.5)$$

where $\mathbf{n}$, the Frank director, is a unit vector specifying the direction of the principal axis (or the average direction of ordering) and

$$S = \frac{1}{2}\langle 3(\nu \cdot \mathbf{n})^2 - 1\rangle. \qquad (2.6)$$

In the intermediate phase of C_{70}, the equilibrium state is spatially uniform and $\mathbf{n}$ points along one of the threefold axes of the fcc lattice. Let the three axes of the cubic lattice be X, Y, and Z. Thus, in the cubic coordinates, $n_X^2 = n_Y^2 = n_Z^2 = \frac{1}{3}$ and the diagonal components of Q_{ij} in this basis are zero.

Since the Q_{ij} is traceless it has only five independent components, say, Q_1, Q_2, Q_3, Q_4, and Q_5. If they are defined so that

$$\mathrm{Tr}Q^2 = \sum_{i=1}^5 Q_i^2, \qquad (2.7)$$

where Tr is the trace operation, then it is possible to define five symmetric and traceless 3×3 matrices I_{ij}^α such that

$$Q_{ij} = \sum_{\alpha=1}^5 I_{ij}^\alpha Q_\alpha. \qquad (2.8)$$

From Eq. (2.7) and Eq. (2.8) it follows that

$$\sum_{i,j} I_{ij}^\alpha I_{ij}^\beta = \delta^{\alpha,\beta}, \qquad (2.9)$$

$$\sum_\alpha I_{ij}^\alpha I_{kl}^\alpha = \frac{1}{2}\left(\delta_{ik}\delta_{jl} + \delta_{il}\delta_{jk} - \frac{2}{3}\delta_{ij}\delta_{kl}\right). \qquad (2.10)$$

The last relation uses the fact that the trace with respect to the pairs (i, j) and (k, l) must be zero. Explicit constructions of these matrices are given later.

B. Landau free energy

We are ultimately interested in obtaining a phenomenological theory for the dynamical fluctuations of the C_{70} order parameter. To do this we construct, from the order parameter, a Landau-Ginzburg-Wilson free energy functional F_Q. F_Q consists of quantities made up of combinations of the order parameter components that are invariant under the symmetry operations of the cubic lattice (the high-temperature disordered phase). Obviously, all the rotationally invariant quantities can belong to F_Q. Thus we can decompose it as

$$F_Q = F_I + F_A, \qquad (2.11)$$

where F_I is the isotropic, i.e., rotationally invariant, part and F_A is the anisotropic part, which is invariant only under the symmetry elements of the fcc lattice. F_I is identical to the free energy for nematic liquid crystals[29] and is given by

$$F_I = n \int d^3x \left(\frac{r}{2}\mathrm{Tr}(Q^2) - f\sqrt{\frac{2}{3}}\mathrm{Tr}(Q^3) + \frac{e}{4}[\mathrm{Tr}(Q^2)]^2 \right.$$
$$\left. + \frac{C}{2}(\nabla_i Q_{ij})(\nabla_k Q_{kj}) + \frac{D}{2}(\nabla_i Q_{jk})(\nabla_i Q_{jk})\right), \qquad (2.12)$$

where $r = a(T - T_0)$ changes sign at temperature T_0 and Tr denotes a trace over the tensor indices. The coefficients a, A, D, f, e, and C are functions of temperature whose temperature dependence may be neglected when discussing phenomena at temperatures near T_0. We use the summation convention whereby a sum over repeated indices is assumed. We have included invariant terms only up to fourth order in the order parameter since we hope to apply this theory only close to the transition where we assume the order parameter is small. We retain terms only to second order in the gradient operator because we are interested only in the long-wavelength limit where the details of the lattice are not important. Since the lattice constant is $a = 14.39$ Å, our theory is valid only for wave vectors k such that $ak \ll 1$ or $k \ll 0.5$ Å^{-1}.

At high temperatures F_I favors $S = 0$. At sufficiently low temperatures it favors nonzero S at wave vector $\mathbf{k} = 0$, but does not prefer any particular direction for $\mathbf{n}$. Thus we would see Goldstone modes (broken symmetry modes) associated with fluctuations in the director of $\mathbf{n}$ (as in nematic liquid crystals). The existence of the third-order term implies that the transition is first order in nature; the order parameter undergoes a discontinuous jump in value at the transition. In the future we use $C = 0$, to simplify the resulting equations of motion. As more data become available, one might refine the theory by allowing C to be nonzero, including additional second-order anisotropic gradient terms reflection cubic symmetry, and allowing the coefficients in Eq. (2.12) and in Eq. (2.14), below, to have a temperature dependence. However, our aim here is to obtain a qualitatively correct theory which is as simple as possible.

The lowest-order contribution[21] to F_A is of order Q^2. It can be written in various ways. Let $\mathbf{e}^X$, $\mathbf{e}^Y$, and $\mathbf{e}^Z$ be unit vectors along the X, Y, and Z cubic crystal axes, respectively. We define

$$I_{ijkl} = \sum_{\alpha = X,Y,Z} e_i^\alpha e_j^\alpha e_k^\alpha e_l^\alpha. \tag{2.13}$$

Then

$$F_A = \frac{nA}{2} \int d^3x (I_{ijkl} Q_{ij} Q_{kl} - \mathrm{Tr} Q^2) \tag{2.14a}$$

$$= \frac{nA}{2} \int d^3x (Q_{XX}^2 + Q_{YY}^2 + Q_{ZZ}^2 - \mathrm{Tr} Q^2) \tag{2.14b}$$

$$= -A\, n \int d^3x (Q_{XY}^2 + Q_{YZ}^2 + Q_{ZX}^2). \tag{2.14c}$$

If Q_{ij} is uniaxial, then F_A can be expressed in terms of S and $\mathbf{n}$ as

$$F_A = \frac{A}{2} nS^2 \int d^3x \left[\left(n_X^2 - \frac{1}{3} \right)^2 + \left(n_Y^2 - \frac{1}{3} \right)^2 \right.$$
$$\left. + \left(n_Z^2 - \frac{1}{3} \right)^2 - \frac{2}{3} \right]. \tag{2.15}$$

This shows clearly that for $A > 0$, $n_X^2 = n_Y^2 = n_Z^2 = \frac{1}{3}$ defines the lowest-energy directions, which are the four (111) directions. Similarly, the (100) directions are the highest-energy directions. Of course, for $A < 0$, the role of these two extremal directions are interchanged.

C. Representations of Q

We have already shown that it is possible to define 3×3 matrices $\mathbf{I}^\alpha$ so that $Q_{ij} = \sum_\alpha I_{ij}^\alpha Q_\alpha$. The exact form of the matrices $\mathbf{I}$ is determined by convenience and the coordinate system in use.

We pick a coordinate system such that the z axis is along the equilibrium direction of $\mathbf{n}$ in the ordered phase. We call this the rhombohedral system since the z axis is along the threefold axis of the rhombohedral lattice. The rhombohedral coordinate axes are given in terms of the cubic axes by $\mathbf{e}^x = \frac{1}{\sqrt{6}}(1,1,-2)$, $\mathbf{e}^y = \frac{1}{\sqrt{2}}(-1,1,0)$, and $\mathbf{e}^z = \frac{1}{\sqrt{3}}(1,1,1)$. A natural choice for the five matrices I_{ij}^α in the isotropic case ($A = 0$) is

$$\mathbf{I}^1 = \frac{1}{\sqrt{6}} \begin{pmatrix} -1 & 0 & 0 \\ 0 & -1 & 0 \\ 0 & 0 & 2 \end{pmatrix} , \quad \mathbf{I}^2 = \frac{1}{\sqrt{2}} \begin{pmatrix} 1 & 0 & 0 \\ 0 & -1 & 0 \\ 0 & 0 & 0 \end{pmatrix} , \quad \mathbf{I}^3 = \frac{1}{\sqrt{2}} \begin{pmatrix} 0 & 1 & 0 \\ 1 & 0 & 0 \\ 0 & 0 & 0 \end{pmatrix} , \tag{2.16}$$

$$\mathbf{I}^4 = \frac{1}{\sqrt{2}} \begin{pmatrix} 0 & 0 & 1 \\ 0 & 0 & 0 \\ 1 & 0 & 0 \end{pmatrix} , \quad \mathbf{I}^5 = \frac{1}{\sqrt{2}} \begin{pmatrix} 0 & 0 & 0 \\ 0 & 0 & 1 \\ 0 & 1 & 0 \end{pmatrix} . \tag{2.17}$$

Then

$$Q_1 = \sqrt{\frac{3}{2}} Q_{zz} , \quad Q_2 = \frac{\sqrt{2}}{3} \eta = \frac{1}{\sqrt{2}}(Q_{xx} - Q_{yy}), \tag{2.18}$$

$$Q_3 = \sqrt{2} Q_{xy} , \quad Q_4 = \sqrt{2} Q_{zx} , \quad Q_5 = \sqrt{2} Q_{yz}. \tag{2.19}$$

In the ordered state, the mean value of Q_1, the uniaxial order parameter, is nonzero while the remaining variables have a mean value of zero. Also Q_2 is the biaxial order parameter, Q_4 and Q_5 measure rotations of $\mathbf{n}$ away from the preferred direction, and Q_3 measures the direction of biaxial order. Unfortunately, in the rhombohedral system F_A is very complicated, as can be calculated using Eq. (2.14),

$$F_A = -\frac{A}{12} \left\{ 9 Q_{zz}^2 + [\sqrt{2}(Q_{xx} - Q_{yy}) + 2Q_{zx}]^2 \right.$$
$$\left. + 4(\sqrt{2} Q_{xy} - Q_{yz})^2 \right\}, \tag{2.20}$$

and the choice of I's given above does not simplify it. A natural choice of variables in this case, which diagonalizes F_A, is

$$Q_a = \sqrt{\frac{2}{3}}(\sqrt{2} Q_{xy} - Q_{yz}), \tag{2.21a}$$

$$Q_b = \sqrt{\frac{2}{3}}(\sqrt{2} Q_{yz} + Q_{xy}), \tag{2.21b}$$

$$Q_c = \sqrt{\frac{1}{6}}(\sqrt{2}(Q_{xx} - Q_{yy}) + 2Q_{zx}), \tag{2.21c}$$

$$Q_d = \sqrt{\frac{1}{6}}((Q_{xx} - Q_{yy}) - 2\sqrt{2} Q_{zx}), \tag{2.21d}$$

$$Q_e = \sqrt{\frac{3}{2}} Q_{zz}. \tag{2.21e}$$

The corresponding I's are

$$\mathbf{I}^a = \sqrt{\frac{2}{3}}\mathbf{I}^3 - \frac{1}{\sqrt{3}}\mathbf{I}^5 \ , \quad \mathbf{I}^b = \sqrt{\frac{2}{3}}\mathbf{I}^5 + \frac{1}{\sqrt{3}}\mathbf{I}^3 \ , \quad \mathbf{I}^c = \sqrt{\frac{2}{3}}\mathbf{I}^2 + \frac{1}{\sqrt{3}}\mathbf{I}^4, \tag{2.22}$$

$$\mathbf{I}^d = -\sqrt{\frac{2}{3}}\mathbf{I}^4 + \frac{1}{\sqrt{3}}\mathbf{I}^2 \ , \quad \mathbf{I}^e = \mathbf{I}^1. \tag{2.23}$$

Now Q_a, Q_b, Q_c, and Q_d measure a combination of rotation of $\mathbf{n}$ and development of biaxial order. With this choice we have

$$F_A = -\frac{A}{2}\ n\ \int d^3x\ \ \left(Q_e^2 + Q_a^2 + Q_c^2\right), \tag{2.24}$$

$$\begin{aligned}
F_I = \int d^3x\ \ n\ &\left[\frac{r}{2}\sum_{\alpha=a}^{e} Q_\alpha^2 + \frac{e}{4}\left(\sum_{\alpha=a}^{e} Q_\alpha^2\right)^2 - \frac{D}{2}\sum_{\alpha=a}^{e} Q_\alpha \nabla^2 Q_\alpha \right. \\
&- \frac{f}{3}\left(Q_e^3 + \frac{1}{\sqrt{2}}Q_c^3 + Q_d^3\right) + f\ \sqrt{2}\left(Q_e Q_a Q_b + Q_e Q_c Q_d - \frac{1}{\sqrt{2}}Q_a Q_b Q_c\right) \\
&\left. + \frac{f}{2}(Q_e Q_c^2 + Q_e Q_a^2 + Q_c^2 Q_d - 2Q_b^2 Q_d + \sqrt{2}Q_a^2 Q_c - Q_a^2 Q_d) \right], \tag{2.25}
\end{aligned}$$

where in the gradient term we have performed a partial integration.

D. Thermodynamics

The free energy $F_Q = F_A + F_I$ can be used to determine the order parameter as a function of temperature, the latent heat of the transition, the order parameter susceptibility, and metastability temperature.[30] Here we will be content with a mean-field analysis that ignores fluctuations. We will compare the mean-field forms for the above quantities with their experimentally determined (or estimated) values to obtain estimates for the phenomenological parameters a, T_0, A, etc., of our theory.

First, we note from Eqs. (2.24) and (2.25) that the system becomes locally unstable to the development of a nonzero order parameter Q_e when $r - A$ becomes zero. Since $r = a(T - T_0)$, this instability occurs at $T = T^*$, where

$$T^* = T_0 + A/a. \tag{2.26}$$

If we let Q_0 be the equilibrium value of Q_e, then its value is determined by the equation of state

$$\left.\frac{\delta F}{\delta Q_e}\right|_{Q_e=Q_0} = 0 = Q_0(r - A - fQ_0 + eQ_0^2). \tag{2.27}$$

At the first-order transition, defined to occur when $T = T_c$, the free energies of the ordered and disordered phases are both zero so that

$$\left(\frac{1}{2}(r - A) - \frac{1}{3}fQ_0(T_c) + \frac{1}{4}eQ_0^2(T_c)\right)Q_0^2(T_c) = 0, \tag{2.28}$$

where $Q_0(T_c)$ is the mean-field value of Q_0 at the transition. Equations (2.27) and (2.28) determine T_c and $Q_0(T_c)$ to be

$$Q_0(T_c) = \frac{2f}{3e}, \tag{2.29}$$

$$T_c = \frac{2f^2}{9ae} + T^*. \tag{2.30}$$

This results indicates that the difference between T_c (where the thermodynamic transition occurs) and T^* (which is the limit of metastability on cooling) is of order $f^2/(ae)$. If T^{**} is the limit of metastability of the ordered phase on heating, then $T^{**} - T_c$ is also of order $f^2/(ae)$. The *latent heat (L)* of the phase transition is $T\Delta S$, where ΔS is the jump in entropy that accompanies the transition and is given by

$$\begin{aligned}
L = T_c\Delta S = \ &T_c\left(\frac{\partial F}{\partial T}\right)_{(T-T_c)\to 0_+} \\
&-T_c\left(\frac{\partial F}{\partial T}\right)_{(T-T_c)\to 0_-} \tag{2.31} \\
= \ &\frac{1}{2}anT_c\int d^3r Q_0^2(\mathbf{r}) = \frac{1}{2}aNT_cQ_0^2, \tag{2.32}
\end{aligned}$$

where we have assumed that the predominant temperature dependence near the transition is contained in r and N is the number of molecules in the system.

The order parameter susceptibilities are easily calculated via

$$\chi_{\alpha\beta}^{-1}(\mathbf{x},\mathbf{x}') = \frac{\delta^2 F}{\delta Q_\alpha(\mathbf{x})\ \delta Q_\beta(\mathbf{x}')}. \tag{2.33}$$

Above T_c, in the disordered state, the Fourier transform $\chi_{\alpha\beta}^{-1}(\mathbf{k})$ of this susceptibility is diagonal with entries

$$\begin{aligned}
\chi_{aa}^{-1} = \chi_{cc}^{-1} &= \chi_{ee}^{-1} \\
&= n(r - A + Dk^2) = n[a(T - T^*) + Dk^2], \tag{2.34}
\end{aligned}$$

$$\chi_{bb}^{-1} = \chi_{dd}^{-1} = n(r + Dk^2) = n[a(T - T_0) + Dk^2]. \tag{2.35}$$

Below T_c, in the ordered state, Q_a and Q_b couple to each other but are decoupled from other Q's. Q_c and Q_d are

similarly coupled to each other and decoupled from the other Q's and Q_e remains independent. We have

$$\chi^{-1}(a,b) = \chi^{-1}(c,d)$$
$$= \begin{pmatrix} n(2fQ_0 + Dk^2) & \sqrt{2}nfQ_0 \\ \sqrt{2}nfQ_0 & n(A + fQ_0 + Dk^2) \end{pmatrix},$$
$$\tag{2.36}$$

$$\chi_{ee}^{-1} = n(-fQ_0 + 2eQ_0^2 + Dk^2). \tag{2.37}$$

Note that when $A = 0$, $\det[\chi^{-1}(a,b)] \sim Dk^2$ as $k \to 0$ as required by rotational invariance of the mean-field ground state. We recall that in the classical limit of interest to us here, the susceptibility $\chi_{\alpha,\beta}$ is linearly proportional to the fluctuations in Q_α,

$$S_{\alpha\beta}(\mathbf{k}) = \int d^3x \langle \delta Q_\alpha(x) \delta Q_\beta(x') \rangle e^{-i\mathbf{k} \cdot (x-x')} \tag{2.38}$$

$$= k_B T \chi_{\alpha,\beta}(\mathbf{k}), \tag{2.39}$$

where $\delta Q_\alpha = Q_\alpha - \langle Q_\alpha \rangle$ and k_B is the Boltzmann constant. In evaluating the Fourier transform use has been made of the fact that the system must be translationally invariant, at least in the long-wavelength limit where the lattice can be ignored.

E. Numerical estimates of the coefficients

We will now fix the unknown coefficients in our free energy by fitting the predictions of our theory to experimental results. From the NMR response width at T_c we can determine $Q_0(T_c)$. The constants a, f, A, and e can be fixed using $Q_0(T_c)$ and the experimental value of the latent heat of the transition. D can be determined either from the width of the diffusion peak above T_c or from the range and strength of interactions between the molecules. The value of moment of inertia can be calculated from the geometry of the molecule. The lattice constant of the cubic phase is $c = 14.39$ Å. We will express the coefficients in terms of these constants and the number density of the molecules in the solid (n). The results are collected in Table I.

TABLE I. Values of various constants.

Constant	Value (experimental)
c (Å)	14.39
a	$204k_B$
f	$20k_B T_c$
Q_0 (T_c)	0.1
e	$136k_B T_c$
A	$27k_B T_c$
T_c (K)	300
T_0 (K)	259
T^* (K)	299
D	$20c^2 k_B T_c$
I_0	$1360\ n\hbar^2/(k_B T_c)$
n	$4/c^3$

1. Transition temperature (T_c)

Depending on the experiment chosen[31,19,20] the value of T_c ranges from 300 K to 340 K. We choose, for our calculations,

$$T_c = 300 \text{ K}. \tag{2.40}$$

2. Order parameter at the transition, $Q_0(T_c)$

In the ordered state, the NMR reponse width of a powder sample is a direct measure of the order parameter as shown in Eq. (5.5). If this is studied close to the transition temperature, we can establish Q_0 at T_c. From our Eq. (5.5), below, we know that the width of the NMR absorption line is given, as a fraction of the original resonance frequency for ^{13}C, by $\frac{3}{2}\sqrt{\frac{3}{2}}\sigma_0' Q_0(T)$, where $(1-\sigma_0')$ is the factor to which the magnetic field is renormalized by the screening. Tycko et al.[32] find $\sigma_0' \approx 45 \times 10^{-6}$ and the width is approximately 65–70 $\times 10^{-6}$. This gives $Q_0(T) \approx 0.8$ as compared to the zero-temperature value of 0.82. But since these measurements were made in the fully ordered low-temperature state, we do not consider them further. Sprik et al.[25] have suggested a model based on their molecular dynamics simulations. In the high-temperature phase, the long axes of the molecules point with equal probability along the six face diagonals. In the intermediate phase the orientation of the long axes of the molecules is distributed such that on average they point along the threefold axis of the rhombohedral lattice, but their angular distribution is peaked at an angle of 18° with respect to the threefold axis. Blinc et al.[31] have used a variant of this model to explain their NMR results. In their model the long axes of the molecules are allowed to point along one of the six face diagonals of the cubic lattice [(110), (011), (101), (1$\bar{1}$0), (01$\bar{1}$), and ($\bar{1}$01)] in the high-temperature phase. In the intermediate phase, they have two sets, consisting of three axes each, along which the long axes of the molecules can point. The first set consists of three directions oriented at an angle ϵ with respect to the threefold axis and the second set consists of three directions prependicular to the threefold axis. The two sets are occupied with probabilities, $(1 + P)/2$ and $(1 - P)/2$. In the high-temperature regime the six directions coincide with the face diagonals of the cube. The order parameter as defined by us (they also choose the same order parameter) would then become a function of both the angle ϵ and P which is a measure of how they favor the occupation of the first set of directions over the second. In the fcc phase, $\epsilon = \cos^{-1}\sqrt{\frac{2}{3}} \approx 35.5$. In the intermediate phase, $Q_{zz} = \frac{1+P}{2}\cos^2 \epsilon - \frac{1}{3}$. Using their values of $P = 0.3$ and $\epsilon = 35.5$ close to the transition we get

$$Q_0(T_c) = \sqrt{3/2}Q_{zz} = \sqrt{3/2}(P/3) = 0.12. \tag{2.41}$$

For our calculations we choose

$$Q_0(T_c) = 0.1. \tag{2.42}$$

3. Determination of a

From the experimentally determined latent heat (L) of the transition we can determine a using Eq. (2.32). There are two experiments to consider. Grivei et al.[23] report a value of 2.2 J/g for the latent heat of the transition and T_c of 340 K and Vaughan et al.[19] report a value of 3.6 J/g and $T_c = 345$ K. We choose a latent heat of 3 J/g for our calculations. Using the density (1.74 g/cc), we find that the latent heat per unit volume is $L = 8.7 \times 10^6$ J m^{-3}. The density also tells us that the number density n of C_{70} molecules in the solid is

$$n = 1.237 \times 10^{27} \text{ m}^{-3}. \tag{2.43}$$

Thus we have, from Eq. (2.32),

$$(a/k_B) = (2L)/[k_B T_c Q_0^2(T_c)n] \approx 200 \tag{2.44}$$

for $T_c \approx 300$ K and $Q_0(T_c) \approx 0.1$.

4. Determination of A

Some muon spin resonance experiments[27,33] detect the effects of the cubic anisotropy in the motions of the molecules at an anisotropy temperature T_a, which is about 40 K above the transition temperature, so that $T_a = T_c + 40$ K. This means that we can estimate the value of A to be approximately

$$A \approx a(T_a - T_c) = 200k_B(40\text{K}) = 27k_B T_c . \tag{2.45}$$

5. Determination of T^*

For the Landau expansion to be valid around the transition temperature, $T_c - T^*$ should be small. Experimentally, the difference in transition temperatures observed in a cooling versus a heating experiment is less than 5°.[24] Thus a reasonable value is $(T_c - T^*) \approx 1$ K and for this choice we get

$$T_0 = 259 \text{ K}, \tag{2.46}$$

since $T^* = T_0 + A/a$. Choosing a smaller value of T^* or a larger value for $T_c - T^*$ makes the order parameter relatively more insensitive to the temperature close to the transition. So, if the order parameter were carefully measured close to the transition, the value of T^* could be fixed quite easily.

6. Static mean-field determination of f, e

From Eq. (2.29) and Eq. (2.30) we have

$$e = 2a(T_c - T^*)/Q_0^2(T_c) = 133k_B T_c, \tag{2.47}$$

$$f = 3eQ_0(T_c)/2 = 20k_B T_c. \tag{2.48}$$

7. Determination of D

There are two methods of estimating the size of the constant D. The first method uses the range (R) and strength (U) of the interactions between the molecules. The strength of the interaction between two molecules is of the order of aT^*/z, where $z = 12$ is the number of nearest neighbors. The range is approximately the lattice constant $c = 15$ Å. Thus,

$$D \approx UR^2 \approx aT^* c^2/z = 20k_B T_c c^2. \tag{2.49}$$

The second method uses the width of the non-Bragg (or diffuse) peaks of neutron scattering experiments in the disordered state. These measurements have not been performed. The width of the x-ray and neutron diffuse peaks is inversely proportional to the correlation length. Thus, the width of the peak is given by $\sqrt{\frac{a(T - T_0)}{D}}$. From the value of D estimated above we would predict a diffuse peak width of about 0.15 Å^{-1}.

8. Calculation of I_0

The moment of inertia I_0' of the molecule is determined by its geometry.[28] We find that

$$I_0' = 1.43 \times 10^{-43} \text{ K g}^2 = 1360\frac{\hbar^2}{k_B T_c}, \tag{2.50}$$

$$I_0 = nI_0', \tag{2.51}$$

where I_0 is the moment of inertia density.

III. DYNAMICS

A. Phenomenological equations of motion

In this section, we will derive the phenomenological dynamical equations for the C_{70} order parameter Q_{ij} valid at long wavelength and low frequency. Long-wavelength hydrodynamical modes, with frequencies that tend to zero with wave number $\mathbf{k}$, are determined entirely by conservation laws and broken continuous symmetries. In the absence of anisotropy, angular momentum $\mathbf{L}$ is conserved. In addition there are two variables Q_{zx} and Q_{yz}, describing broken rotational symmetry. When anisotropy is included, angular momentum is no longer conserved and the modes associated with broken rotational symmetry are no longer hydrodynamic. We will assume, however, that all modes associated with the order parameter Q_{ij} and $\mathbf{L}$ are slow compared to microscopic relaxation times at long wavelengths. Our dynamical theory must, therefore, include angular momentum as well as Q_{ij} and our equations of motion will contain nondissipative Poisson bracket couplings between $\mathbf{L}$ and Q_{ij}. These are the couplings responsible for librons in the low-temperature nondissipative limit.

The microscopic dynamical variables of our model are the angle variables $\theta(1)$ and $\phi(1)$ for each molecule (the

Euler angles) and their associated canonically conjugate momenta,

$$p_\theta = I'_0 \dot{\theta}(1), \qquad (3.1)$$

$$p_\phi = I'_0 \sin^2[\theta(1)] \dot{\phi}(1), \qquad (3.2)$$

where I'_0 is the moment of inertia of the C$_{70}$ molecule about the axes perpendicular to its long axis. The angular momentum of the molecule is

$$\mathbf{L}(1) = p_\theta \hat{e}_\phi - \frac{1}{\sin\theta} p_\phi \hat{e}_\theta, \qquad (3.3)$$

where $\hat{e}_\phi$ and $\hat{e}_\theta$ are the usual unit vectors on a sphere. We can now introduce an angular momentum density

$$\mathbf{L}(\mathbf{r}) = \sum_l \mathbf{L}(1)\delta(\mathbf{r} - 1). \qquad (3.4)$$

The long-wavelength kinetic energy is then

$$F_K = \frac{1}{2I} \int d^3x \mathbf{L}^2(x), \qquad (3.5)$$

where $I = nI'_0$. The effective free energy is

$$H = F_K + F_Q. \qquad (3.6)$$

The phenomenological equations of motion for Q_{ij} and $\mathbf{L}$ can be written as

$$\frac{\partial Q_{ij}(x)}{\partial t} = \int d^3x' [Q_{ij}(x), L_k(x')] \frac{\delta H}{\delta L_k(x')}$$
$$- \Gamma^Q_{ijkl} \frac{\delta H}{\delta Q_{kl}(x)}, \qquad (3.7)$$

$$\frac{\partial L_i(x)}{\partial t} = \int d^3x' [L_i(x), Q_{kj}(x')] \frac{\delta H}{\delta Q_{kj}(x')}$$
$$+ \gamma^L_{ijkl} \nabla_j \nabla_k \frac{\delta H}{\delta L_l(x)} + \Gamma^L_{ij} \frac{\delta H}{\delta L_j}. \qquad (3.8)$$

Here

$$[Q_{ij}(\mathbf{x}), L_k(\mathbf{x}')] = \sum_{\alpha,1} \left(\frac{\partial Q_{ij}(\mathbf{x})}{\partial q^\alpha(1)} \frac{\partial L_k(\mathbf{x}')}{\partial p^\alpha(1)} \right.$$
$$\left. - \frac{\partial Q_{ij}(\mathbf{x})}{\partial p^\alpha(1)} \frac{\partial L_k(\mathbf{x}')}{\partial q^\alpha(1)} \right) \qquad (3.9)$$

$$= \delta(\mathbf{x} - \mathbf{x}') [\epsilon_{ikl} Q_{jl}(\mathbf{x}) + \epsilon_{jkl} Q_{il}(\mathbf{x}')], \qquad (3.10)$$

where $q^\alpha = (\theta, \phi)$ and $p^\alpha = (p_\theta, p_\phi)$ is the Poisson bracket of $Q_{ij}(\mathbf{x})$ with $L_k(\mathbf{x}')$. Γ^Q_{ijkl} is a dissipative tensor. It must be symmetric and traceless in ij and kl. In a cubic environment, there can in general be two independent constants in Γ^Q_{ijkl}. To simplify our analysis we will use the form appropriate to an isotropic system with a single constant:

$$\Gamma^Q_{ijkl} = \frac{1}{2}\Gamma_Q \left(\delta_{ik}\delta_{jl} + \delta_{il}\delta_{jk} - \frac{2}{3}\delta_{ij}\delta_{kl} \right). \qquad (3.11)$$

γ^L_{ijkl} and Γ^L_{ij} are also dissipative tensors. In the absence of anisotropy, $\mathbf{L}$ is conserved and Γ^L is zero and

$$\gamma^L_{ijkl} = \gamma\delta_{jk}\delta_{il}. \qquad (3.12)$$

In the presence of anisotropy (A nonzero), $\mathbf{L}$ is not conserved and Γ^L_{ij} is strictly speaking nonzero. If it is assumed that the microscopic Γ^L_{ij} is zero, then mode coupling will produce a Γ^L_{ij} that is of order A^2. We will assume that

$$\Gamma^L_{ij} = \gamma^L \delta_{ij}. \qquad (3.13)$$

To calculate the mode structure, it is convenient to re-express Eq. (3.7) and Eq. (3.8) in terms of the five independent variables $Q_a, \ldots, Q_e$ of Q_{ij}. Using the identities

$$\frac{\delta Q_{ij}(x)}{\delta Q_{kl}(x')} = \delta(x - x')\frac{1}{2} \left(\delta_{ik}\delta_{jl} + \delta_{il}\delta_{jk} - \frac{2}{3}\delta_{ij}\delta_{kl} \right),$$
$$(3.14)$$

$$I^\alpha_{ij} Q_{ij} = Q_\alpha, \qquad (3.15)$$

we get

$$\frac{\delta H}{\delta Q_{ij}(x)} = \int d^3x' \frac{\delta H}{\delta Q_\alpha(x')} \frac{\delta Q_\alpha(x')}{\delta Q_{ij}(x)}$$
$$= I^\alpha_{kl} \int d^3x' \frac{\delta H}{\delta Q_\alpha(x')} \frac{\delta Q_{kl}(x')}{\delta Q_{ij}(x)}$$
$$= I^\alpha_{ij} \frac{\delta H}{\delta Q_\alpha(x)}. \qquad (3.16)$$

Using these relations, it is straightforward to rewrite Eq. (3.7) and Eq. (3.8) as

$$\frac{\partial Q_\alpha(\mathbf{r},t)}{\partial t} = \int d^3r' \ [Q_\alpha(\mathbf{r},t), L_i(r')] \frac{\delta H}{\delta L_i(r')}$$
$$- \Gamma_Q \frac{\delta H}{\delta Q_\alpha(\mathbf{r},t)}, \qquad (3.17)$$

$$\frac{\partial L_i(\mathbf{r},t)}{\partial t} = \int d^3r' \ [L_i(\mathbf{r},t), Q_\alpha(r')] \frac{\delta H}{\delta Q_\alpha(r')}$$
$$- (\gamma^L - \gamma\nabla^2) \frac{\delta H}{\delta L_i(\mathbf{r},t)}. \qquad (3.18)$$

These are the equations governing the long-wavelength dynamics of $\mathbf{L}$ and Q_{ij}. They are nonlinear equations which could in principle be used to calculate the effects of mode-mode coupling.

To obtain the dynamical modes to harmonic level, we linearize Eq. (3.17) and Eq. (3.18). These linearized equations can be written as

$$\hat{M}_{\alpha,\beta}(\mathbf{k}, \partial_t)\delta X_\alpha(\mathbf{k}, t) = 0, \qquad (3.19)$$

where $\delta X_\alpha = (\delta Q_a, \ldots, \delta Q_e, \delta L_x, \ldots, \delta L_z)$ is the complete set of eight independent variables and $\partial_t = \frac{\partial}{\partial t}$. The equations for δX_α (and the matrix $\hat{M}_{\alpha,\beta}$) decompose into two independent equations for Q_e and L_z and two sets of equivalent equations for the triads Q_a, Q_b, and L_x and Q_c, Q_d, and L_y:

$$M_{ee}(\mathbf{k}, \partial_t)\delta Q_e = \left(\partial_t + \Gamma_Q \chi_{ee}^{-1}\right)\delta Q_e = 0, \qquad (3.20)$$

$$M_{L_z, L_z}(\mathbf{k}, \partial_t)\delta L_z = [\partial_t + \Gamma_L(k)/I]\delta L_z = 0, \qquad (3.21)$$

$$M_{\alpha,\beta}(\mathbf{k}, \partial_t)\delta X_\beta^{(1)} = 0, \qquad (3.22)$$

$$M_{\alpha,\beta}(\mathbf{k}, \partial_t)\delta X_\beta^{(2)} = 0, \qquad (3.23)$$

where

$$\Gamma_L(k) = \gamma^L + \gamma k^2, \qquad (3.24)$$

$$\delta X_\alpha^{(1)} = (\delta Q_a, \delta Q_b, \delta L_x), \qquad (3.25)$$

$$\delta X_\alpha^{(2)} = (\delta Q_c, \delta Q_d, \delta L_y), \qquad (3.26)$$

$$M_{\alpha,\beta}(\mathbf{k}, \partial_t) = \begin{pmatrix} \partial_t + \Gamma_Q \chi_{aa}^{-1} & +\Gamma_Q \chi_{ab}^{-1} & -I^{-1}Q_0 \\ +\Gamma_Q \chi_{ab}^{-1} & \partial_t + \Gamma_Q \chi_{bb}^{-1} & \sqrt{2}I^{-1}Q_0 \\ Q_0 Dk^2 & -\sqrt{2}Q_0(Dk^2 + A) & \partial_t + \Gamma_L(k)/I \end{pmatrix}. \qquad (3.27)$$

These equations predict modes with respective frequencies $\omega_e = -i\Gamma_Q \chi_{ee}^{-1}$ and $\omega_z = -i\Gamma_L(k)/I$ for Q_e and L_z. Imaginary frequencies correspond to purely dissipative modes. The other mode frequencies are determined by $\det M(\mathbf{k}, \omega) = 0$. In the isotropic phase this gives

$$\omega_a = \omega_c = \omega_e = -i\Gamma_Q \chi_{aa}^{-1}, \qquad (3.28)$$

$$\omega_b = \omega_d = -i\Gamma_Q \chi_{bb}^{-1}. \qquad (3.29)$$

In the ordered phase, there are two sets of three coupled modes. The frequencies of these modes, in terms of the coefficients of the free energy, are quite complicated. They can, however, be calculated analytically in two limits, which we will now consider.

1. Isotropic limit (A = 0)

In this limit we expect the real parts of the mode frequencies to go to zero in the limit $\mathbf{k} = 0$ since the propagating modes must be Goldstone modes. There are two modes each at frequencies ω_1^0 and ω_2^0 and a dissipative mode at ω_3^0 and their values are given by

$$\omega_{1,2}^0 = \frac{-i}{2}\left(\Gamma_Q nDk^2 + \gamma k^2/I\right)$$
$$\pm \frac{1}{2}\sqrt{12Q_0^2 k^2 nD/I - (\Gamma_Q nDk^2 - \gamma k^2/I)^2}, \qquad (3.30)$$

$$\omega_3^0 = -i\Gamma_Q \left(nDk^2 + 3nfQ_0\right). \qquad (3.31)$$

The superscript 0 denotes the isotropic case. ω_3^0 is the frequency associated with biaxial fluctuations and is nonzero. Since we are interested only in the small $\mathbf{k}$ limit we can simplify the expressions above to give

$$\omega_{1,2}^0 = \frac{-i}{2}\left(\Gamma_Q nDk^2 + \gamma k^2/I\right) \pm Q_0 k\sqrt{3nD/I}, \qquad (3.32)$$

$$\omega_3^0 = -i\Gamma_Q(nDk^2 + 3nfQ_0). \qquad (3.33)$$

There is one mode at $\omega = -i\Gamma_Q \chi_{ee}^{-1}$ corresponding to Q_e and another at $\omega = -i\gamma k^2/I$ corresponding to L_z. Because we have not included any anisotropy, the librons (i.e., $\omega_{1,2}^0$) have a dispersion relation quite similar to that of phonons, namely, $\omega \propto k$ with k^2 damping for each of the allowed modes of oscillation.

2. Small dissipation: Small anisotropy limit

In this limit, $\Gamma_Q \chi_{ab}^{-1} \ll \Gamma_Q \chi_{aa}^{-1}$, $\Gamma_Q \chi_{bb}^{-1} \ll \sqrt{nA/I}$ (where $\chi_{bb}^{-1} = \chi_{aa}^{-1} + nA$), and $\Gamma_Q nA \ll \Gamma_Q \chi_{aa}^{-1}$, and we have

$$\omega_1 = -i\left(\frac{1}{2}[\Gamma_L(k)/I + \Gamma_Q \chi_{aa}^{-1}] - nA\Gamma_Q \frac{Dk^2 + A}{3Dk^2 + 2A}\right) + \frac{1}{2}\sqrt{Q_0^2(12nDk^2 + 8nA)/I - [\Gamma_L(k)/I - \Gamma_Q \chi_{aa}^{-1}]^2}, \qquad (3.34)$$

$$\omega_2 = -i\left(\frac{1}{2}[\Gamma_L(k)/I + \Gamma_Q \chi_{aa}^{-1}] - nA\Gamma_Q \frac{Dk^2 + A}{3Dk^2 + 2A}\right) - \frac{1}{2}\sqrt{Q_0^2(12nDk^2 + 8nA)/I - [\Gamma_L(k)/I - \Gamma_Q \chi_{aa}^{-1}]^2}, \qquad (3.35)$$

$$\omega_3 = -i\Gamma_Q \chi_{aa}^{-1} - inA\Gamma_Q \frac{Dk^2}{3Dk^2 + 2A}. \qquad (3.36)$$

The Q_e mode remains at $\omega = -i\Gamma_Q \chi_{ee}^{-1}$, but the L_z mode becomes $\omega = -i\Gamma_L(k)/I$, which does not go to zero with $\mathbf{k}$ because $\mathbf{L}$ is no longer conserved in the anisotropic limit. We see that in the presence of anisotropy the li-

brons are no longer phononlike but have a nonzero frequency at $k = 0$. The argument of the square root can become negative for some range of temperatures if the damping is too large or the order parameter Q_0 is too
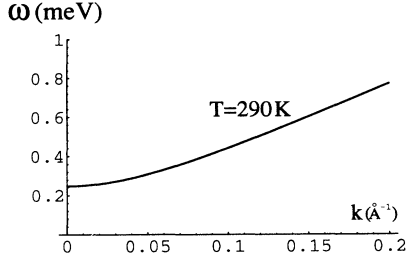
FIG. 3. Variation of the real part of the propagating mode frequency $\omega^0_{1,2}$ versus wave vector for the underdamped case at $T = 290$ K $< T_c$. For this case we took $\Gamma_Q = 100$ (J sec)$^{-1}$, $\gamma = 10^{-28}$ m^2/sec, $\gamma^L = 0$, and the other parameters as given in Table I.

small, in which case the librons are overdamped. If Q_0 is large enough, then the librons are well-defined excitations with a frequency at $k = 0$ $Q_0\sqrt{2nA/I}$.

Figure 3 shows the dispersion relation obtained for the values of the constants determined in the section on thermodynamics. Figure 4 shows the variation of the frequency of the propagating mode with temperature for different choices of damping.

B. Dynamic structure factor

1. Phenomenological model

The dynamic correlation function for δX_p and δX_q is defined as

$$S_{pq}(\mathbf{r},\mathbf{r}',t,t') = \langle \delta X_p(\mathbf{r},t)\delta X_q(\mathbf{r}',t')\rangle. \quad (3.37)$$

Neutron scattering measures the Fourier transform of S_{pq} defined by

$$S_{pq}(\mathbf{k},\omega) = \int_{-\infty}^{\infty} d^3(x-x') \int_{-\infty}^{\infty} d(t-t')\ S_{pq}(x,x',t,t')$$
$$\times e^{i\{\omega(t-t')-\mathbf{k}\cdot(\mathbf{x}-\mathbf{x}')\}}, \quad (3.38)$$

where p,q represent the order parameter variables. This is then related to the dissipative part of the response functions $\chi''_{\alpha,\beta}(\mathbf{k},\omega)$ via the fluctuation dissipation theorem, which in the classical limit of interest to us here is

$$S_{\alpha,\beta}(\mathbf{k},\omega) = \frac{2k_BT}{\omega}\chi''_{\alpha,\beta}(\mathbf{k},\omega). \quad (3.39)$$

The dynamic response function $\chi_{\alpha,\beta}(\mathbf{k},z)$ is related in the usual way[34] to the matrix $\hat{M}_{\alpha,\beta}(\mathbf{k},-iz)$ by

FIG. 4. Variation of the real part of the propagating mode frequency $\omega^0_{1,2}$ versus temperature for $k = 0.1$ Å^{-1} and for $\gamma = 5 \times 10^{-28}$ m^2/sec and $\gamma^L = 0$. The straight line is the underdamped case, for which $\Gamma_Q = 180$ (J sec)$^{-1}$. The dashed line is the overdamped case, for which $\Gamma_Q = 300$ (J sec)$^{-1}$. Note the discontinuity for the underdamped case at the first-order transition at $T_c = 300$ K.

$$\hat{M}^{-1}_{\alpha,\beta}(\mathbf{k},-iz) = \frac{1}{iz}\left[\chi_{\alpha,\gamma}(\mathbf{k},z) - \chi_{\alpha,\gamma}(\mathbf{k})\right]\chi^{-1}_{\gamma,\beta}(\mathbf{k}). \quad (3.40)$$

Thus

$$S_{\alpha,\beta}(\mathbf{k},\omega) = 2[\hat{M}^{-1}_{\alpha,\gamma}(\mathbf{k},-i(\omega+i\epsilon))$$
$$+ \hat{M}^{-1}_{\alpha,\gamma}(\mathbf{k},-i(\omega-i\epsilon))]S_{\gamma,\beta}(\mathbf{k}), \quad (3.41)$$

where $S_{\gamma,\beta}(\mathbf{k}) = \int \frac{d\omega}{2\pi} S_{\gamma,\beta}(\mathbf{k},\omega) = k_BT\chi_{\gamma,\beta}(\mathbf{k})$ is the instantaneous correlation function.

In the disordered phase, all modes are decoupled and dissipative, and

$$S_{\alpha,\beta}(\mathbf{k},\omega) = S_{\alpha,\alpha}(\mathbf{k},\omega)\delta_{\alpha,\beta} = \frac{2\Gamma_Qk_BT}{\omega^2 + (\Gamma_Q\chi^{-1}_{\alpha,\alpha})^2}\delta_{\alpha,\beta}. \quad (3.42)$$

We can give an explicit expression for the correlations in the ordered phase in the limit of small dissipation that we discussed earlier in the calculation of the mode frequencies ($\Gamma_Q\chi^{-1}_{ab} \ll \Gamma_Q\chi^{-1}_{aa}, \Gamma_Q\chi^{-1}_{bb} \ll \sqrt{nA/I}$, $\chi^{-1}_{bb} = \chi^{-1}_{aa} + nA$, and $\Gamma_QnA \ll \Gamma_Q\chi^{-1}_{aa}$). Let us define the following quantities so that it is easy to express the correlation (we only give $\langle\delta Q_a\delta Q_a\rangle$ here):

$$\lambda_0 = \Gamma_Q\chi^{-1}_{aa} + nA\Gamma_Q\frac{Dk^2}{3Dk^2+2A}, \quad (3.43)$$

$$\lambda_1 = \Gamma_Q\chi^{-1}_{aa} + \Gamma_L(k)/I - nA\Gamma_Q\frac{Dk^2+A}{3Dk^2+2A}, \quad (3.44)$$

$$\omega_0 = \sqrt{Q_0^2(12nDk^2+8nA)/I - [\Gamma_Q\chi^{-1}_{aa} - \Gamma_L(k)/I]^2}, \quad (3.45)$$

where ω_0 is the frequency of the propagating mode and λ_0 and λ_1 represent the dissipation of the modes. Using these expressions we have

$$S_{aa}(\mathbf{k},\omega) = k_BT\chi_{aa}\left(\frac{2Dk^2+2A}{(3Dk^2+2A)}\right)\frac{2\lambda_0}{\omega^2+\lambda_0^2} + 2k_BT\chi_{aa}\frac{Dk^2}{3Dk^2+2A}\frac{\lambda_0(\omega^2-\omega_0^2)}{(\omega^2-\omega_0^2)^2+4\omega^2\lambda_1^2}$$
$$\times 2k_BT\chi_{aa}\frac{Dk^2}{3Dk^2+2A}\frac{2\lambda_1(\omega_0^2)}{(\omega^2-\omega_0^2)^2+4\omega^2\lambda_1^2}. \quad (3.46)$$
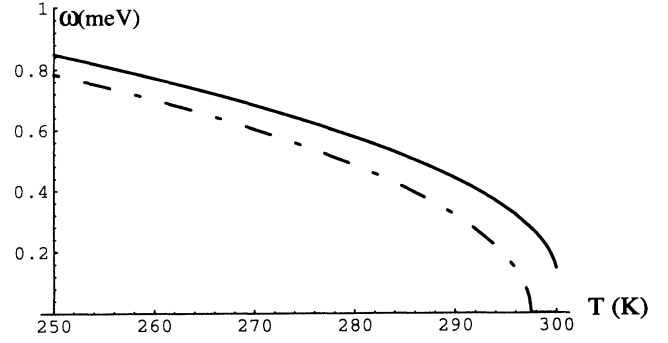
2. Diffusion model

We can also calculate the dynamic correlations using the diffusion model. We will compare the two approaches here. The diffusion model assumes that the C_{70} molecules act as independent rotors at each site. Each rotor undergoes a rotational random walk with diffusion constant $D_\parallel$ for rotations about the long axis and $D_\perp$ for rotations perpendicular to the long axis. If we ignore the spinning degree of freedom, the molecule is the diffusion analog of the symmetric top problem in quantum mechanics. This model ignores all interactions among the molecules. It cannot distinguish between the ordered and disordered phases, and, in particular, it does not predict the existence of low-temperature librons. It, nonetheless, is a useful model for the high-temperature phase.

We are interested in evaluating correlations of the form

$$C_{mn}(t) \equiv \sum_{i,j=1}^{70} \langle Y_2^m(\hat{r}_i, t)_s^* Y_2^n(\hat{r}_j, t=0)_s \rangle , \qquad (3.47)$$

where the subscript s on the spherical harmonics indicates that it is evaluated in a system of coordinates fixed in space and the angle brackets indicate an average over the canonical probability distribution. In terms of body fixed (B) coordinates (in which the z axis lies along the

fivefold axis of the molecule) we may write

$$Y_2^m(\hat{r}_i, t)_s = \sum_\alpha D_{m,\alpha}^{(2)}(\Omega_{s\to b})^* Y_2^\alpha(\hat{r}_i)_b , \qquad (3.48)$$

where $\Omega_{s\to b}$ denotes the triad of Euler angles which takes the space fixed axes into the body fixed axes. For the C_{70} molecule we set

$$\sum_{i=1}^{70} Y_2^\alpha(\omega_i)_b^* = \sigma_\alpha . \qquad (3.49)$$

Due to the symmetry of the molecule, only σ_0 is nonzero. Furthermore,

$$C_{mn}(t) = \int p(\Omega_{s\to b}(t), \Omega_{s\to b}(0)) p(\Omega(0))$$

$$\times \sum_{\alpha\beta} D_{m\alpha}^{(2)}(\Omega_{s\to b}(t)) D_{n\beta}^{(2)}(\Omega_{s\to b}(0))^* \sigma_\alpha^* \sigma_\beta , \qquad (3.50)$$

where $p(\Omega(0))$ is the probability that the orientation at $t = 0$ is $\Omega(0)$ and $p(\Omega(t), \Omega(0))$ is the probability that the orientation at time t is $\Omega(t)$ given that it was $\Omega(0)$ at $t = 0$. This conditional probability is the Green's function discussed in Appendix C. Also $p(\Omega(0)) = 1/(8\pi^2)$. So

$$C_{mn}(t) = \sum_{\alpha\beta} \sigma_\alpha^* \sigma_\beta \int d\Omega_t \int d\Omega_0 \sum_{LMN} \frac{2L+1}{(8\pi^2)^2} D_{m\alpha}^{(2)}(\Omega_t) D_{n\beta}^{(2)}(\Omega_0)^* D_{MN}^{(L)}(\Omega_t)^* D_{MN}^{(L)}(\Omega_0) e^{-\lambda_{LMN} t/a_0}$$

$$= \delta_{mn} \frac{1}{5} \sum_N |\sigma_N|^2 e^{-\lambda_{2mN} t/a_0} = \frac{\delta_{mn}}{5} \sigma_0^2 e^{-\lambda_{2m0} t/a_0} = \frac{\delta_{mn}}{5} \sigma_0^2 e^{-6D_\perp t}, \qquad (3.51)$$

where

$$\lambda_{LMN} = L(L+1)D_\perp + N^2(D_\parallel - D_\perp), \qquad (3.52)$$

where $D_\parallel$ and $D_\perp$ are orientational diffusion constants proportional to $I_\parallel^{-1}$ and $I_\perp^{-1}$, respectively. Using the definitions $Q_a, \ldots, Q_e$ given in Eq. (4.5), Eq. (4.6), and Eq. (4.7) we get the correlations for the order parameters:

$$S_{ab}(\omega) = \delta_{ab} \frac{2}{15} \frac{6D_\perp}{\omega^2 + (6D_\perp)^2}. \qquad (3.53)$$

This result for the correlation function is identical to that predicted within our model in the isotropic limit ($A = 0$) when interactions between molecules are ignored so that one can make the identifications (a) $\Gamma_Q \chi_{aa}^{-1} = 6D_\perp$ and (b) $\frac{15}{2} an(T - T_0) = k_B T$. Note that although the hydrodynamic and diffusion approaches represent quite different approximations, they nevertheless lead to similar results. The fact that we studied a Y_2^M correlation function [see Eq. (3.47)] limited the sum over L in Eq. (3.51) to $L = 2$. A more general correlation function (as is needed to interpret neutron scattering) requires a sum over L. Then, $S_{ab}(\omega)$ will be the sum over a large number of Lorenztian line shapes each of which has a different width. On the other hand, the hydrodynamic result, Eq. (3.42), has only a single Lorentzian, whose

width, however, is temperature dependent. These calculations incorporate quite different physics: The diffusion model, by its complete neglect of correlations between adjacent molecules, is restricted to a very large wave vector, whereas the hydrodynamic model is valid in just the opposite limit.

IV. NEUTRON SCATTERING

The cross section for coherent neutron scattering at wave vector $\mathbf{k}$ and energy ω is given by

$$I_{coh}(\mathbf{k}, \omega) \propto \frac{k_{in}}{k_{out}} \int \langle e^{i\mathbf{k}\cdot\mathbf{r}_i(t)} e^{-i\mathbf{k}\cdot\mathbf{r}_j(0)} \rangle e^{i\omega t} dt, \qquad (4.1)$$

which is the Van Hove relation.[36] We can calculate this quantity using our theory. To evaluate I_{coh} we use

$$e^{i\mathbf{k}\cdot\mathbf{r}} = 4\pi \sum_{l=0}^\infty i^l j_l(kr) \sum_{m=-l}^l Y_l^{m*}(\hat{\mathbf{k}}) Y_l^m(\hat{\mathbf{r}}). \qquad (4.2)$$

We can either use the symmetric top diffusion model, discussed earlier, or our phenomenological model of the dynamics.

A. Phenomenological model

This is the model we have proposed. It gives us a unified description of the system above and below the transition. We use Eq. (4.2) in the expression for S_{coh} and sum over all the atoms in the solid. The coordinate of the nth atom on the pth molecule can be written as $\mathbf{r} = \mathbf{r}_{np} + \mathbf{R}_p$,

where $\mathbf{r}_{np}$ is the coordinate of the atom with respect to the center of the molecule and $\mathbf{R}_p$ is the coordinate of the center of the molecule with respect to the origin. $|\mathbf{r}_{np}|$ and $\mathbf{R}_p$ are independent of time in our model since we ignore the inter- and intramolecular phonons. We choose the coordinate system to be along the crystal axes. Carrying out the expansion, we obtain

$$\langle e^{i\mathbf{k}\cdot\mathbf{r}(t)} e^{-i\mathbf{k}\cdot\mathbf{r}(0)} \rangle = \frac{(4\pi)^2}{N} \sum_{p,p'} \sum_{n,n'} \sum_{l,l'} \sum_{m,m'} e^{i\mathbf{k}\cdot(\mathbf{R}_p - \mathbf{R}_{p'})} \langle j_l(kr_{np}) j_{l'}(kr_{n'p'}) Y_l^m(\hat{\mathbf{r}}_{np}(0)) Y_{l'}^{m'*}(\hat{\mathbf{r}}_{n'p'}(t)) \rangle$$
$$\times Y_l^{m*}(\hat{\mathbf{k}}) Y_{l'}^{m'}(\hat{\mathbf{k}}). \tag{4.3}$$

We make the approximation of keeping only terms with $l \leq 2$ since in the hydrodynamic limit ($k \ll 0.5$ Å) the higher-order terms do not make an appreciable contribution.

Since the various l moments are not correlated with one another (that is, $l = 2$ is not correlated to $l = 0$ terms) in our theory, we can separate the $l = 0$ and $l = 2$ terms. Since we are ignoring the phonons, the $l = 0$ term contributes only to static scattering, i.e., $\delta(\omega)$, and yields the Bragg peaks, i.e., $\delta(\mathbf{k} - \mathbf{G})$ peaks ($\mathbf{G}$ is a reciprocal lattice vector). We are interested in the intensity at $\mathbf{k} \neq \mathbf{G}$ for information on dynamics.

We can consider the spinning molecule to be made up of five structures of the form shown in Fig. 9 below. It is shown in Appendix A that for a given molecule the sum over n can be converted to a sum over the five structures indexed by α so that $\sum_i j_2(kr_i) Y_2^m(\hat{r}_n) = \mathcal{F}(k) Y_2^m(\hat{\nu})$, where ν is the direction of the long axis of the molecule and $\mathcal{F}(k) = \sum_\alpha g(\alpha) j_2(kr_\alpha)$. The geometrical constant $g(\alpha)$ is defined in Appendix C. Thus,

$$\langle e^{i\mathbf{k}\cdot\mathbf{r}(t)} e^{-i\mathbf{k}\cdot\mathbf{r}(0)} \rangle = \frac{(4\pi)^2}{N} \mathcal{F}^2(k) \sum_{p,p'} \sum_{m,m'=-2}^{2} e^{i\mathbf{k}\cdot(\mathbf{R}_p - \mathbf{R}_{p'})} \langle Y_2^m(\hat{\nu}(\mathbf{R}_p, t = 0)) Y_2^{m'*}(\hat{\nu}(\mathbf{R}_{p'}, t)) \rangle$$
$$\times Y_2^{m*}(\hat{\mathbf{k}}) Y_2^{m'}(\hat{\mathbf{k}}). \tag{4.4}$$

The Y_l^m's in the equation above can now be expressed in terms of the order parameters of our theory. The sum over p, p' results in giving us the Fourier transforms at $\mathbf{k}$ of the correlation functions of the order parameters. We also perform a temporal Fourier transform to get the intensity as a function of $\mathbf{k}$ and ω.

We need to average over the directions of $\mathbf{k}$ since we are interested in the results of powder experiments (the qualitative results remain the same for single-crystal experiments). The correlations involve only the magnitude of the wave vector so that the integration over directions of $\mathbf{k}$ will involve only the averages of the spherical harmonics of $\mathbf{k}$. Using the orthogonality of the Y_l^m's and the definitions

$$Y_2^2(\hat{\nu}) = \sqrt{\frac{15}{32\pi}} (Q_{xx} - Q_{yy} + 2iQ_{xy})$$
$$= \sqrt{\frac{5}{16\pi}} [\sqrt{2}Q_c + Q_d + i(Q_b + \sqrt{2}Q_a)], \tag{4.5}$$

$$Y_2^1(\hat{\nu}) = -\sqrt{\frac{15}{8\pi}} (Q_{zx} + iQ_{yz}) = -\sqrt{\frac{5}{16\pi}} [Q_c - \sqrt{2}Q_d + i(-Q_a + \sqrt{2}Q_b)], \tag{4.6}$$

$$Y_2^0(\hat{\nu}) = \sqrt{\frac{5}{16\pi}} 3Q_{zz} = \sqrt{\frac{15}{8\pi}} Q_e, \tag{4.7}$$

we can simplify Eq. (4.4) to get

$$I(\mathbf{k}, \omega) \propto 30\pi \frac{k_{out}}{k_{in}} \mathcal{F}^2(k) [S_{aa}(\mathbf{k}, \omega) + S_{bb}(\mathbf{k}, \omega)$$
$$+ S_{cc}(\mathbf{k}, \omega) + S_{dd}(\mathbf{k}, \omega) + S_{ee}(\mathbf{k}, \omega)], \tag{4.8}$$

where k_{in}, k_{out} are the wave vectors of the incoming and outgoing neutrons, respectively. Note that off-diagonal terms in $S_{\alpha\beta}(k, \omega)$ do not contribute although they would in a single crystal. We can calculate the scattering intensity as a function of ω at a particular $\mathbf{k}$ for various values of dissipation using the values for the coefficients that we estimated in the previous section. The value of Γ_Q controls the height and width of the peak at $\omega = 0$ while both Γ_Q and γ control the height and width of the peak belonging to the propagating mode. Figures 5, 6, and 7 show the neutron scattering cross section, calculated from our theory, as a function of ω at $k = 0.1$ Å^{-1} for different temperatures. They show how the increase in ordering leads to well-defined peaks. For these figures the dissipation constants have been chosen to be

$$\gamma = 5 \times 10^{-28} \text{ m}^2/\text{sec}, \quad \Gamma_Q = 600 \text{ (J sec)}^{-1}, \quad \gamma^L = 0. \tag{4.9}$$

Actual measurements of the peak widths should constrain these constants. We cannot extend the formulas given above to large values of $\mathbf{k}$, such as those used in Refs. 26 and 35, since our theory is valid only for small $k \ll 0.5$ Å^{-1}.

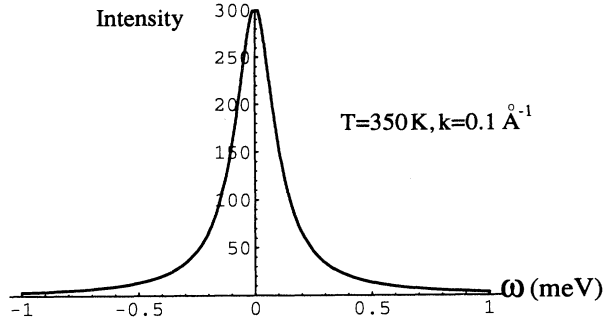FIG. 5. Neutron scattering cross section predicted by the phenomenological theory $T = 350$ K $> T_c = 300$ K, with the parameters given in Eq. (4.9) and Table I.

FIG. 6. Neutron scattering cross section predicted by the phenomenological theory $T = 295$ K $< T_c = 300$ K, with the parameters given in Eq. (4.9) and Table I.

B. Diffusion model

This model is designed to be valid at large k where we may consider each molecule to be executing rotational diffusion independent of its neighbor. Thus, we need to evaluate the expression

$$\langle e^{i\mathbf{k}\cdot\mathbf{r}_i(t)}e^{-i\mathbf{k}\cdot\mathbf{r}_j(0)}\rangle = \frac{1}{N}\sum_{i,j=1}^{70}\int d\Omega_0\int d\Omega p(\Omega,\Omega_0,t)$$
$$\times p(\Omega_0)e^{i\mathbf{k}\cdot\mathbf{r}_i(t)}e^{-i\mathbf{k}\cdot\mathbf{r}_j(0)}, \qquad (4.10)$$

where r_i is the position of atom i relative to the center of the molecule and $N = 70$ the number of atoms. We can evaluate this using the expansion of Eq. (4.2) and Eq. (3.51). Without loss of generality we can have the space

fixed Z axis along $\mathbf{k}$, since the lattice is irrelevant in this model. Then

$$e^{i\mathbf{k}\cdot\mathbf{r}_i} = 4\pi\sum_l i^l j_l(kr_i)\sqrt{\frac{2l+1}{4\pi}}\sum_m D_{0m}^{l*}(\Omega(t))Y_l^m(\omega_i),$$
$$(4.11)$$

where Ω is the time-dependent angular coordinates of the body fixed axes with respect to the space fixed axes and ω is the angular coordinate of the atom with respect to the body fixed axes. In Appendix C we give a derivation of $p(\Omega,\Omega_0,t)$ which enables the evaluation of Eq. (4.10). Thereby we get the well-known[26,35] result

$$S(k,t) = \frac{k_{\rm in}}{k_{\rm out}}\sum_{l=1}^{\infty}\sum_{i,j=1}^{70}(4\pi)^2 j_l(kr_i)j_l(kr_j)\sum_{m=-l}^{l}Y_l^{m*}(\omega_i)Y_l^m(\omega_j)e^{[-m^2(D_{\parallel}-D_{\perp})t-l(l+1)D_{\perp}t]}. \qquad (4.12)$$

To compare with our hydrodynamic model we will limit this model to small k. Then only the smallest values of l are important. The $l = 1$ and $l = 3$ terms do not contribute because of the symmetry of the molecule. Thus the most important contribution comes from the $l = 2$ term and the rest can be ignored without substantially altering the results. The body fixed z axis is a fivefold axis of symmetry, and so only $m = 5n \leq l$ (n is an integer) contribute. Taking the temporal Fourier transform of Eq. (4.12) we get

$$I_{\rm coh}(\mathbf{k},\omega) \approx \frac{2\tau}{1+(\omega\tau)^2}\frac{k_{\rm in}}{k_{\rm out}}\sum_{i,j=1}^{70}(4\pi)^2 j_l(kr_i)j_2(kr_j)$$
$$\times Y_2^{0*}(\omega_i)Y_2^0(\omega_j), \qquad (4.13)$$

where $1/\tau = 6D_1$. We have already discussed, Sec III, the limit in which this result approaches the isotropic high-temperature result of the phenomenological theory.

Here we discuss various simple limits of this model. The most obvious limit, and one that works reasonably
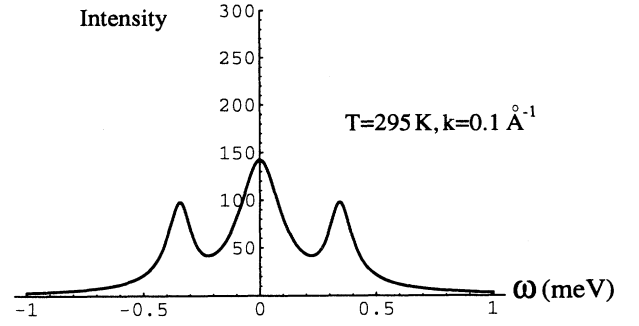
well, is the isotropic limit in which $D_{\perp} = D_{\parallel}$. This limit described the orientational diffusion of a sphere. Obviously, it is better to use the more complete theory of Eq. (4.12). To emphasize the fact that the molecule is a
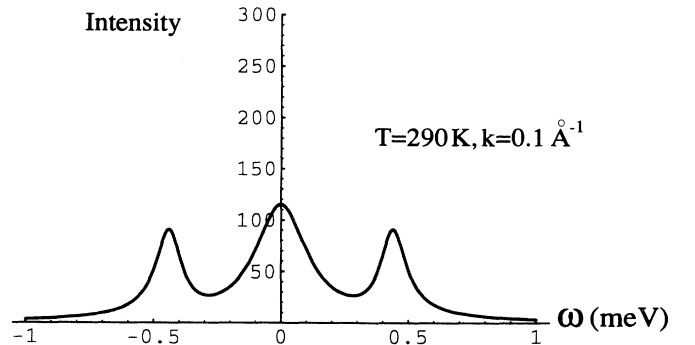

FIG. 7. Neutron scattering cross section predicted by the phenomenological theory for $T = 290$ K $< T_c = 300$ K, with the parameters given in Eq. (4.9) and Table I.

prolate ellipsoid one may assume that $I_\parallel \ll I_\perp$ or that $D_\parallel \gg D_\perp$. In the literature[26,35] this has been done by setting $D_\perp = 0$ in a limit called "uniaxial" diffusion. By that, it is meant that diffusion takes place around the fivefold axis, but the fivefold axis itself remains fixed in space. This approximation seems to us to be an implausible one, and indeed the data does not support it.[26] If it desired to fit the data with a single parameter, a more appealing approximation would be to set $D_\parallel = \infty$, i.e., to assume that the spinning motion is very rapid, so that the diffusive width in the neutron scattering reflects, not the rotations about the fivefold axis, but rather the diffusive motion of the fivefold axis itself. In particular, this picture fits in with the idea that the cubic to rhombohedral transition is one in which the diffusive motion of the fivefold axis is becoming nearly hydrodynamic, whence effectively $D_\parallel = \infty$. Apparently, this approximation ($D_\parallel = \infty$) was not used to interpret the experiments of Refs. 26 and 35. Ultimately, we hope that the data will be refined so as to allow a determination of *both* $D_\parallel$ and $D_\perp$.

V. NMR

Since ^{12}C has no magnetic moment it is impossible to do NMR studies on a sample with only this isotope present. Thus, we require the existence of ^{13}C, which has a nuclear magnetic moment, for these studies. The natural abundance of ^{13}C is quite low, which means that the probability that two ^{13}C isotopes will occur on a given C_{70} molecule is very small, and we may assume that no more than one ^{13}C occurs on any molecule. The nucleus of ^{13}C does not have an electric quadrupole moment. Hence, the only magnetic effect, other than the field applied, is the magnetic field due to the orbital motion of electrons (the chemical shift). We derive the expression for the shift of the NMR frequency due to the chemical shift and show how the density of states at different frequencies in a powder sample, due to the shift, gives us information on the order parameter. We also calculate T_1, due to chemical shift effects, from our theory.

A. Chemical shifts

Chemical shifts occur due to the electrons in the environment of the nucleus with the magnetic moment. The analysis given here follows Munowitz.[37] There is a magnetic field ($\mathbf{B'}$) at the nucleus due to the electron cloud in the presence of a magnetic field (diamagnetism). The resultant field need not be parallel to the applied field. This is reflected by choosing $\mathbf{B'} = \sigma \cdot \mathbf{B}$, where σ is the diamagnetic shielding tensor. The Hamiltonian for the nuclear moment in the magnetic field is given by

$$H = -\gamma_n \hbar \mathbf{I} \cdot \mathbf{B} + \gamma_n \hbar \mathbf{I} \cdot \sigma \cdot \mathbf{B}, \tag{5.1}$$

where the sign implies that the electrons act to screen out the $\mathbf{B}$ field. Since the molecule is spinning about the long axis, in the molecular frame we must have

$$\langle \sigma \rangle = \begin{pmatrix} \sigma_1 & 0 & 0 \\ 0 & \sigma_1 & 0 \\ 0 & 0 & \sigma_2 \end{pmatrix}, \tag{5.2}$$

where $\langle\ \rangle$ indicates an average over the orientation motion. The value of σ_1, σ_2 obviously depends on the molecular site under consideration. We can rewrite $\langle \sigma \rangle$ in the form shown below, following the standard approach,[37]

$$\langle \sigma \rangle = \left(\frac{2}{3}\sigma_1 + \frac{1}{3}\sigma_2 \right) \begin{pmatrix} 1 & 0 & 0 \\ 0 & 1 & 0 \\ 0 & 0 & 1 \end{pmatrix}$$

$$+ \frac{2}{3}(\sigma_2 - \sigma_1) \begin{pmatrix} -\frac{1}{2} & 0 & 0 \\ 0 & -\frac{1}{2} & 0 \\ 0 & 0 & 1 \end{pmatrix}. \tag{5.3}$$

The first part is a uniform shift irrespective of the magnetic fields orientation and can be absorbed in the definition of the Larmor frequency.

B. Order parameter

The second, anisotropic, part of the tensor leads to a shift in the Larmor frequency that depends on the degree of ordering (the size of the order parameter) of the molecules in the solid. This can be used to directly measure the order parameter by studying the response width of an NMR experiment performed on a powder sample, as we shall soon show. This is a static phenomenon.

If the consequence is worked through then it is found that the resonance line shape is determined by

$$P(\nu) = \frac{1}{2} \int_{-1}^{1} d(\cos \Theta_B)\ \delta \left(\nu - \nu_0 + \frac{2}{3} P_2(\cos \Theta_B)\Delta\nu \right), \tag{5.4}$$

where $\Delta\nu = (3/2)\sqrt{3/2}Q_0 \sigma_0' \nu_0$. Thus,

$$P(\nu) = \begin{cases} \frac{1}{2\sqrt{(\Delta\nu)(\nu - \nu_0 - (\Delta\nu)/3)}} \\ \qquad \text{for}\ \Delta\nu > 3(\nu - \nu_0) > -2\Delta\nu, \tag{5.5} \\ 0 \quad \text{otherwise.} \tag{5.6} \end{cases}$$

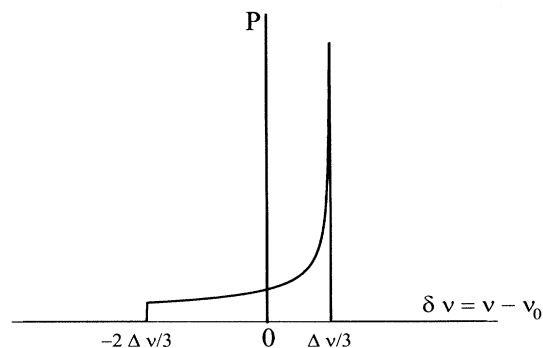Figure 8 shows the frequency dependence of $P(\nu)$. De-

FIG. 8. $P(\nu)$, the resonance line shape, calculated from the phenomenological theory according to Eq. (5.5).

termination of the line width $\Delta\nu$ then leads to a determination of Q_0.

C. T_1: The longitudinal relaxation time

T_1 is the time constant of relaxation of the magnetic moment in the **B**-field direction to its equilibrium value. We have a spin-$\frac{1}{2}$ nuclear magnetic moment in a magnetic field, which makes it a two-state system. If we have a perturbation that causes transitions between the + and − states, then the transition rates obey the relations $W_{+\to-} = W_{-\to+} = W$. Let the difference in populations be n. Each transition changes this number by 2; thus,

$$\frac{dn}{dt} = -2Wn. \tag{5.7}$$

This can also be derived in a conventional manner. If the state is in equilibrium and the transition rate is slow enough to keep the states in thermal equilibrium on average (the thermal relaxation time is faster than the induced transition rate), then (as shown by Slichter[38]),

$$\frac{1}{T_1} = 2W = 4\pi |\langle \uparrow | H' | \downarrow \rangle|^2 \delta(\omega_\uparrow - \omega_\downarrow - \omega). \tag{5.8}$$

The δ function ensures that absorption occurs only at the the Larmor frequency ($\omega_0 = \omega_\uparrow - \omega_\downarrow$). We can write the perturbation as

$$H' = \gamma_n[I_z B'_z + \tfrac{1}{2}(I_+ B'_- + I_- B'_+)], \tag{5.9}$$

where $\mathbf{B}' = \sigma \cdot \mathbf{B}$. The first term cannot contribute to any decay process but the second term will and can be used to calculate the consequent decay rate. We then have

$$\frac{1}{T_1} = 2W = \gamma_n^2 \left\langle \frac{1}{2} \int B'_+(t) B'_-(0) e^{i\omega_0 t} dt \right\rangle. \tag{5.10}$$

The states are defined with respect to the magnetic field which is defined to be along the z axis of the laboratory coordinate frame. Let us define the intermediate crystal coordinates such that its axes are along the rhombohedral coordinate axes. The angular coordinates of this system with respect to the laboratory system are θ_C, ϕ_C. The molecular coordinate axes are at θ_m, ϕ_m with respect to the intermediate crystal axes. Let the diamagnetic shielding tensor in the molecular system, σ, be given by σ' in the crystal system and σ'' in the laboratory system. Then $B'_+ = (\sigma''_{xz} + i\sigma''_{yz})B_z$ and

$$\frac{1}{T_1} = 2W = \gamma_n^2 \frac{1}{2} \left\langle (\sigma''_{xz} + i\sigma''_{yz})(\sigma''_{xz} - i\sigma''_{yz}) \right\rangle, \tag{5.11}$$

where the correlations are evaluated locally at frequency ω_0. Using the rotation matrices that connect the various coordinate systems we can rewrite the correlations above in terms of the order parameters of our theory. We have

$$\sigma''_{13} + i\sigma''_{23} = \frac{3}{4\sqrt{6}} e^{i\phi_C} \sigma'_0 [\sin 2\theta_C (3Q_e - \sqrt{2}Q_c - Q_d)$$
$$-i2 \sin\theta_C (Q_b + \sqrt{2}Q_a)$$
$$+i2 \cos\theta_C (-Q_a + \sqrt{2}Q_b)$$
$$+2 \cos 2\theta_C (Q_c - \sqrt{2}Q_d)]. \tag{5.12}$$

We are interested in results from powder samples. Each microcrystal in the sample has a fixed alignment with respect to the laboratory axes; that is, θ_C, ϕ_C are not dynamical variables, but, since the orientations are randomly distributed, we must finally perform an average over a random distribution of these variables to get the experimentally observed $\frac{1}{T_1}$. Thus,

$$\left\langle \frac{1}{T_1} \right\rangle = \int_0^{2\pi} \frac{1}{2\pi} d(\phi_C) \int_{-1}^1 \frac{1}{2} d(\cos\theta_C) \frac{1}{T_1(\theta_C, \phi_C)}. \tag{5.13}$$

Using $S_{aa} = S_{cc}$ and $S_{bb} = S_{dd}$ we get

$$\left\langle \frac{1}{T_1} \right\rangle = \frac{9}{40} (\sigma'_0 B\gamma_n)^2 [S_{ee}(\mathbf{r}, \mathbf{r}, \omega_0)$$
$$+2S_{aa}(\mathbf{r}, \mathbf{r}, \omega_0) + 2S_{bb}(\mathbf{r}, \mathbf{r}, \omega_0)]. \tag{5.14}$$

The correlations in the expressions above are local and determined at frequency ω_0. Hence they are given by

$$S_{ii}(r, r, \omega_0) = \int_{k=0}^\Lambda S_{ii}(\mathbf{k}, \omega_0) 4\pi k^2 dk, \tag{5.15}$$

where Λ is a cutoff that we have introduced which is justified by the coarse-grained nature of our effective Hamiltonian.

It can be seen from Eq. (5.14) that T_1 is proportional to the square of the applied magnetic field. This dependence has been verified by Mizugochi et al.[39] The magnetic field comes in due to ω_0 in the correlations but that can be ignored since, for the strength of the fields usually applied in experiments, its contribution is negligible. On the basis of the discussion above we can expect to see a discontinuity in T_1 at the transition. One experiment[32] reports that this does not happen. More investigations are required to verify that this is indeed the case. The decay time is a function of Γ_Q, which is a function of temperature due to mode-mode coupling. In the high-temperature regime, the dependence on Γ_Q is Lorentzian, as shown in Eq. (3.42). It is clear that after performing the wave-vector integration, the value of T_1 diverges for both very small and very large values of Γ_Q. Then T_1 passes through a minimum when the coupling between NMR and the orientational modes is optimal. We have not attempted to determine the dependence of T_1 on temperature through its dependence on Γ_Q, since there seem to be no experimental studies of this effect and the calculations are quite tedious.

VI. CONCLUSIONS

We have given a unified mean-field picture of the statics and dynamics around the high-temperature transition

for C_{70}. The theory is *not* parameter free. We have determined the parameters by calculating the latent heat, neutron scattering cross section, NMR linewidth, and T_1 using our theory. We can suggest a few experiments that can be conducted keeping our theory in mind. The most important ones are the determination of the order parameter as a function of temperature close to the transition determination of the mode frequency for small **k**. Measuring T_1 as a function of temperature might also be considered. It is hoped that this study spurs further investigations in this field.

ACKNOWLEDGMENTS

APPENDIX A: $\sum_I Y_2^M(\hat{R}_I)J_L(KR_I)$ FOR THE SPINNING MOLECULE

When the molecule is spinning about its long axis then it can be modeled as a collection of five structures of the form shown in Fig. 9. All the positions of the atoms in the structure are equidistant from the origin (O, the center of mass of the molecule). Thus,

$$\sum_i Y_2^m(\hat{r}_i)j_2(kr_i) = j_2(kr_\alpha)\sum_i Y_2^m(\hat{r}_i), \qquad (A1)$$

where α indexes the structure and the sum is over positions in the structure α. If the long axis of the molecule, which is along OD, is aligned with the z axis, then, from geometry, we get

$$\sum_i Y_2^m(\hat{r}_i) = g(\alpha)Y_2^m(\hat{\nu}), \qquad (A2)$$

where $\hat{\nu}$ is the direction of the long axis of the molecule and $g(\alpha) = n_\alpha(2L^2 - a^2)/(3L^2 + 3a^2)$. n_α is the number
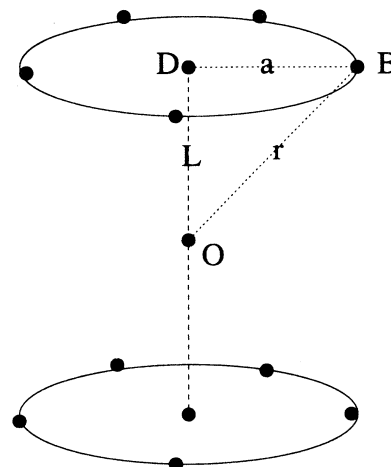

FIG. 9. Shown here is one of the five similar structures of which the molecule is made up when it is spinning about its long axis. The circle could contain either a pentagon or a decagon. In the intermediate phase the atoms are smeared out over this circle.

of atoms in α. Equation (A2) is true even when the long axis of the molecule points in an arbitrary direction since both sides of that equation transform identically under rotations. From the coordinates calculated by Fowler *et al.*[28] we have

$$g(1) = 5.78 , \quad g(2) = 3.11 , \quad g(3) = 1.32,$$
$$g(4) = -4.52 , \quad g(5) = -3.3 .$$

APPENDIX B: POISSON BRACKETS

In this appendix we evaluate a few expressions that are useful writing down the equations of motion.

To evaluate the equations of motion for the dynamical variables we need certain Poisson brackets. From the definitions of the dynamical variables we find

$$[Q_e(x,t), L_i(x',t)] = \delta(x - x') \begin{pmatrix} \sqrt{2}Q_b(x,t) - Q_a(x,t) \\ -Q_c(x,t) + \sqrt{2}Q_d(x,t) \\ 0 \end{pmatrix}, \qquad (B1)$$

$$[Q_a(x,t), L_i(x',t)] = \delta(x - x') \begin{pmatrix} Q_e(x,t) + Q_d(x,t) \\ Q_b(x,t) \\ \sqrt{2}Q_d(x,t) + Q_c(x,t) \end{pmatrix}, \qquad (B2)$$

$$[Q_b(x,t), L_i(x',t)] = \delta(x - x') \begin{pmatrix} -Q_c(x,t) - \sqrt{2}Q_e(x,t) \\ -Q_a(x,t) \\ \sqrt{2}Q_c(x,t) \end{pmatrix}, \qquad (B3)$$

$$[Q_c(x,t), L_i(x',t)] = \delta(x - x') \begin{pmatrix} Q_b(x,t) \\ -Q_d(x,t) + Q_e(x,t) \\ -Q_a(x,t) - \sqrt{2}Q_b(x,t) \end{pmatrix}, \tag{B4}$$

$$[Q_d(x,t), L_i(x',t)] = \delta(x - x') \begin{pmatrix} -Q_a(x,t) \\ -\sqrt{2}Q_e(x,t) + Q_c(x,t) \\ -\sqrt{2}Q_a(x,t) \end{pmatrix}, \tag{B5}$$

where the first element of the column is the result for $i = x$, etc. Below, the transition $\langle Q_e \rangle = Q_0(T)$ which is determined by the equation of state. We get from the Hamiltonian, to linear order in the variables,

$$\frac{\delta H}{\delta Q_\alpha(k)} = \chi_{\alpha,\beta}^{-1} Q_\beta, \tag{B6}$$

where χ^{-1} has been defined in the section on thermodynamics.

APPENDIX C: THE SYMMETRIC TOP AND THE EQUATION OF ANGULAR DIFFUSION

The diffusion equation is of the form

$$\left[\mathcal{L} - a_0 \frac{\partial}{\partial t} \right] \psi(t) = 0, \tag{C1}$$

where $(a_0)^{-1}$ is a diffusion constant and the boundary condition is that $\psi(0)$ is given. For diffusion of a point particle in ordinary Cartesian space, $\mathcal{L} = m^{-1}\nabla^2$ and $\psi(t) \rightarrow \psi(\mathbf{r}, t)$, and D, the usual diffusion constant for which $\langle r^2 \rangle = Dt$, is given by $D \propto (ma_0)^{-1}$. For orientational diffusion of a symmetric top,

$$\hbar^2 \mathcal{L} = \frac{L_x^2 + L_y^2}{I_\perp} + \frac{L_z^2}{I_\parallel}, \tag{C2}$$

where $\mathbf{L}$ is the angular momentum relative to axes $(x, y, \text{and } z)$ fixed in the body, and $I_\perp$ $(I_\parallel)$ is the moment of inertia for rotation around and axis perpendicular (parallel) to the symmetry axis of the body. Then $\psi(t) \rightarrow \psi(\Omega, t)$, where Ω stands for the triad of Euler angles (as defined by Edmonds[41]), α, β, and γ, which take the space fixed coordinate system into a body fixed system. Edmonds gives

$$\mathcal{L} = \frac{1}{I_\parallel} \left(\frac{\partial^2}{\partial \gamma^2} \right) + \frac{1}{I_\perp} \left[\frac{\partial^2}{\partial \beta^2} + \cot \beta \frac{\partial}{\partial \beta} \right.$$
$$\left. + \frac{1}{\sin^2 \beta} \left(\frac{\partial}{\partial \alpha} - \cos \beta \frac{\partial}{\partial \gamma} \right)^2 \right]. \tag{C3}$$

A general solution to this diffusion problem is given by

$$\psi(\Omega, t) = \int d\Omega' G(\Omega, t; \Omega', 0) \psi(\Omega', 0), \tag{C4}$$

where the Green's function satisfies

$$\left[\mathcal{L} + a_0 \frac{\partial}{\partial t} \right] G(\Omega', t'; \Omega, t) = -a_0 \delta(\Omega - \Omega') \delta(t - t'), \tag{C5}$$

with the boundary condition that G vanish for $t' < t$. One has

$$G(\Omega', t'; \Omega, t) = \theta(t' - t) \sum_n \psi_n(\Omega) \psi_n(\Omega')^*$$
$$\times \exp[-(\lambda_n/a_0)(t' - t)], \tag{C6}$$

where $\theta(x) = 1$ for $x > 0$ and is zero otherwise, and the ψ_n's are defined by

$$\mathcal{L}\psi_n(\omega) = -\lambda_n \psi_n(\omega). \tag{C7}$$

These symmetric top eigenfunctions can be found in various sources, several of which, however, have some misprints. An explicit result is given by Edmonds. In our notation (which coincides with that of Rose[40]) one has [correcting his expression for the wave function in the equation preceding his Eq. (4.23)]

$$\psi_{L,M,N}(\omega) = \left(\frac{2L + 1}{8\pi^2} \right)^{1/2} D_{M,N}^{(L)}(\alpha, \beta, \gamma), \tag{C8}$$

$$\lambda_{L,M,N} = \frac{L(L+1)}{I_\perp} + N^2 \left(\frac{1}{I_\parallel} - \frac{1}{I_\perp} \right). \tag{C9}$$

In the limit $I_\parallel = 0$, the solution only involves $D_{M,0}^{(L)}$, a spherical harmonic, which, as expected, does not depend on the Euler angle γ. This reasoning indicates that the solution given in the equation preceding Eq. (4.23) in Rose[40] cannot be correct.

We now replace $\frac{1}{a_0 I_\perp}$ by an appropriate diffusive constant $D_\perp$ and $\frac{1}{a_0 I_\parallel}$ by the diffusive constant $D_\parallel$:

$$G(\Omega', t'; \Omega, t) = \theta(t' - t) \sum_n \frac{2L + 1}{8\pi^2} D_{M,N}^{(L)}(\Omega')^* D_{M,N}^{(L)}(\Omega)$$
$$\times \exp\{-[L(L+1)D_\perp + N^2(D_\parallel - D_\perp)]$$
$$\times (t' - t)\}. \tag{C10}$$

In reference to Eq. (3.51), note that $p(\Omega_{s \rightarrow b}(t), \Omega_{s \rightarrow b}(0)) = G(\Omega_{s \rightarrow b}(t), t; \Omega_{s \rightarrow b}(0), 0)$. We will use the results in this form to carry out the calculation of the coherent neutron scattering cross section for the case of the an object diffusing with two different rates along two different directions.

[1] H. W. Kroto, J. R. Heath, S. C. O'Brien, R. F. Curl, and R. E. Smalley, Nature **318**, 162 (1985).

[2] R. M. Fleming, T. Siegrist, P. M. March, B. Hessen, A. R. Kortan, D. W. Murphy, R. C. Haddon, R. Tycko, G. Dabbagh, A. M. Mujsce, M. L. Kaplan, and S. M. Zahurak, in *Clusters and Cluster-Assembled Materials*, edited by R. S. Averback, J. Bernholc, and D. L. Nelson, MRS Symposia Proceedings No. 206 (Materials Research Society, Pittsburgh, 1991), p. 691.

[3] P. A. Heiney, J. E. Fischer, A. R. McGhie, W. J. Romanow, A. M. Denenstein, J. P. McCauley, Jr., and A. B. Smith III, Phys. Rev. Lett. **66**, 2911 (1991).

[4] R. Sachidanandam and A. B. Harris, Phys. Rev. Lett. **67**, 1467 (1991).

[5] P. A. Heiney, J. E. Fischer, A. R. McGhie, W. J. Romanow, A. M. Denenstein, J. P. McCauley, A. M. Smith III, and D. E. Cox, Phys. Rev. Lett. **67**, 1468 (1991).

[6] S. Liu, Y. J. Lu, M. M. Kappes, and J. A. Ibers, Science **254**, 408 (1991).

[7] W. I. F. David, R. M. Ibberson, J. C. Matthewman, K. Prassides, T. J. Dennis, J. P. Hare, H. W. Kroto, R. Taylor, and D. R. M. Walton, Nature **353**, 147 (1991).

[8] W. I. F. David, R. M. Ibberson, T. J. S. Dennis, J. P. Hare, and K. Prassides, Europhys. Lett. **18**, 219 (1992).

[9] P. A. Heiney, J. Phys. Chem. Solids **53**, 1333 (1992).

[10] A. B. Harris and R. Sachidanandam, Phys. Rev. B **46**, 4944 (1992).

[11] K. H. Michel, J. R. D. Copley, and D. A. Neumann, Phys. Rev. Lett. **68**, 2929 (1992).

[12] R. Heid, Phys. Rev. B **47**, 15912 (1993).

[13] D. A. Neumann, J. R. D. Copley, R. L. Cappelletti, W. A. Kamitakahara, R. M. Lindstrom, K. M. Creegan, D. M. Cox, W. J. Romanow, N. Coustel, J. P. McCauley, N. C. Maliszewskyj, J. E. Fischer, and A. B. Smith, Phys. Rev. Lett. **67**, 3808 (1991).

[14] X. P. Li, J. P. Lu, and R. M. Martin, Phys. Rev. B. **46**, 4301 (1992).

[15] T. Yildirim and A. B. Harris, Phys. Rev. B **46**, 7878 (1992).

[16] J. P. Lu, X. P. Li, and R. M. Martin, Phys. Rev. Lett. **68**, 1551 (1992).

[17] M. Sprik, A. Cheng, and M. L. Klein, J. Phys. Chem. **96**, 2027 (1992).

[18] G. B. M. Vaughan, P. A. Heiney, J. E. Fischer, D. E. Luzzi, D. A. Ricketts-Foot, A. R. McGhie, Yiu-Wing Hui, A. L. Smith, D. E. Cox, W. J. Romanow, R. H. Allen, N. Coustel, J. P. McCauley, Jr., and A. B. Smith III, Science **254**, 1350 (1991).

[19] G. B. M. Vaughan, P. A. Heiney, D. E. Cox, J. E. Fischer, A. R. McGhie, A. L. Smith, R. M. Strongin, M. A. Cichy, and A. B. Smith III, Chem. Phys. **178**, 599 (1993).

[20] C. Christides, I. M. Thomas, T. J. S. Dennis, and K. Pras-

[21] R. Sachidanandam and A. B. Harris, Phys. Rev. B **49**, 2878 (1994).

[22] A. K. Callebaut and K. H. Michel (unpublished).

[23] E. Grivei, B. Nysten, M. Cassart, J-p. Issi, C. Fabre, and A. Rasat, Phys. Rev. B **47**, 1705 (1993).

[24] A. R. McGhie, J. E. Fischer, P. A. Heiney, P. W. Stephens, R. L. Cappelletti, D. A. Neumann, W. H. Mueller, H. Mohn, and H.-U. ter Meer, Phys. Rev. B **49**, 12614 (1994).

[25] M. Sprik, A. Chang, and M. L. Klein, Phys. Rev. Lett. **69**, 1660 (1993).

[26] C. Christides, T. J. S. Dennis, K. Prassides, R. L. Cappelletti, D. A. Neumann, and J. R. D. Copley, Phys. Rev. B **49**, 2897 (1994).

[27] K. Prassides, T. J. S. Dennis, C. Christides, E. Roduner, H. W. Kroto, R. Taylor, and D. R. M. Walton, J. Phys. Chem. **96**, 10600 (1992).

[28] P. W. Fowler, P. Lazzeretti, M. Malagoli, and R. Zanasi, Chem. Phys. Lett. **179**, 174 (1991).

[29] P. G. de Gennes and J. Prost, *The Physics of Liquid Crystals* (Clarendon Press, Oxford, 1993).

[30] N. Goldenfeld, *Lectures on Phase Transitions and the Renormalization Group* (Addison-Wesley, Reading, MA, 1993).

[31] R. Blinc, J. Seliger, J. Dolinsek, and D. Arcon, Solid State Commun. **88**, 9 (1993).

[32] R. Tycko, G. Dabbagh, G. B. M. Vaughan, P. A. Heiney, R. M. Strongin, M. A. Cichy, and A. B. Smith III, J. Chem. Phys. **99**, 7554 (1993).

[33] R. M. Macrae, K. Prassides, I. M. Thomas, E. Roduner, C. Niedermayer, U. Binninger, C. Bernhard, I. A. Hofer, and D. Reid (unpublished).

[34] P. Chaikin and T. C. Lubensky, *Principles of Condensed Matter Physics* (Cambridge Press, Cambridge, England, 1995).

[35] B. Renker, F. Gompf, R. Heid, P. Adelmann, A. Heiming, W. Reichardt, G. Roth, H. Schober, and H. Rietschel, Z. Phys. B **90**, 325 (1993).

[36] S. W. Lovesey, *Theory of Neutron Scattering from Condensed Matter* (Clarendon Press, Oxford, 1994).

[37] M. Munowitz, *Coherence and NMR* (John Wiley and Sons, New York, 1988).

[38] C. P. Slichter, *Principles of Magnetic Resonance*, 3rd ed. (Springer-Verlag, New York, 1992).

[39] K. Mizoguchi, Y. Maniwa, and K. Kume, Mater. Sci. Eng. B **19**, 146, (1993).

[40] M. E. Rose, *Elementary Theory of Angular Momentum* (Wiley, New York, 1957).

[41] A. R. Edmonds, *Angular Momentum in Quantum Mechanics* (Princeton University Press, Princeton, NJ, 1957).

sides, Europhys. Lett. **22**, 611 (1993).